



## Probabilistic modeling and prediction of out-of-plane unidirectional composite lamina properties

Jiaxin Zhang, Michael Shields & Stephanie TerMaath

To cite this article: Jiaxin Zhang, Michael Shields & Stephanie TerMaath (2020): Probabilistic modeling and prediction of out-of-plane unidirectional composite lamina properties, Mechanics of Advanced Materials and Structures, DOI: [10.1080/15376494.2020.1733713](https://doi.org/10.1080/15376494.2020.1733713)

To link to this article: <https://doi.org/10.1080/15376494.2020.1733713>



Published online: 14 Mar 2020.



Submit your article to this journal [↗](#)



Article views: 96



View related articles [↗](#)





View Crossmark data [↗](#)

ORIGINAL ARTICLE



# Probabilistic modeling and prediction of out-of-plane unidirectional composite lamina properties

Jiaxin Zhang<sup>a</sup> , Michael Shields<sup>b</sup> , and Stephanie TerMaath<sup>c</sup> 

<sup>a</sup>Computer Science and Mathematics Division, Oak Ridge National Laboratory, Oak Ridge, Tennessee, USA; <sup>b</sup>Department of Civil Engineering, Johns Hopkins University, Baltimore, Maryland, USA; <sup>c</sup>Department of Mechanical, Aerospace, and Biomedical Engineering, University of Tennessee, Knoxville, Tennessee, USA

## ABSTRACT

Computational simulation provides an efficient means to predict the behavior of customized hybrid material configurations using validated, physics-based models. One limitation to this approach is the quality and quantity of available data to characterize the many constituent input properties. Therefore, a systematic approach to identify the most influential parameters on the hybrid behavior and quantify the corresponding uncertainty in predictive capabilities is required. In this work, an approach using Bayesian multimodel inference and imprecise global sensitivity analysis is presented to investigate the effects of sparse constituent data on the prediction of composite material properties. The methodology allows the identification, using quantified uncertainties, of the most influential constituent material parameters for specified homogenized properties. This sensitivity analysis further enables a dimension reduction when assessing the influence of uncertainties on material properties and can be used to inform testing programs of the constituent properties that require additional testing/data collection in order to minimize uncertainty in macro-scale composite properties. The methodology is specifically demonstrated on the prediction and sensitivity analysis of out-of-plane mechanical properties of a unidirectional lamina.

## ARTICLE HISTORY

Received 9 September 2019  
Accepted 17 February 2020

## KEYWORDS

Uncertainty quantification;  
sensitivity analysis;  
imprecise probability;  
probabilistic prediction;  
carbon fiber;  
dimension reduction

## 1. Introduction

When coupled with Integrated Computational Materials Engineering (ICME) [1], structural design and analysis is advancing toward a simulation environment where engineers can explore materials and hybrid configurations to create optimized parts that meet reliability requirements (Figure 1) [2, 3]. Implementing ICME tools on high-performance computing (HPC) systems and connecting these tools with knowledge databases that store information—such as material properties, boundary and load conditions, and manufacturing data—enables the rapid and seamless investigation of many possibilities of material combinations, manufacturing processes, and configurations. This environment has the potential to enable hybrid material designs with properties customized for a specific application. Including computational tools that perform sensitivity analysis, probabilistic modeling, and optimization further enhances this ICME-based approach by supporting uncertainty quantification and optimized reliability-based design [4–6]. In addition to providing an efficient design and analysis capability, this simulation environment also informs tailored design of experiments that require limited physical testing to fill in knowledge gaps and provide validation data; eliminating the need for all-encompassing and costly experimental testing

programs by focusing physical testing on the most promising materials and configurations.

One potential limitation in this visionary framework is the quantity and quality of the material data in the common library. This library serves as a database to house the material properties, alongside other relevant information and model data, needed for multi-scale analysis and to enable automated input of material properties into models. While many software packages provide such material libraries (for example, COMSOL Multiphysics<sup>®</sup> and MaterialCenter) or offer the capability to manually build one (such as GRANTA MI<sup>™</sup> and Matereality Workgroup DatabasePro), a single, comprehensive experimental program to fully populate all possible properties needed for customized material selection is prohibitive, especially when considering continual dataset expansion due to rapid advances in new material development or hybrid materials consisting of many constituents of varying material type. Given the time and expense of physical testing to fully characterize an ever-increasing, diverse material properties database, the data populating a library is often obtained from disparate sources and of unknown quality. Additionally, some properties may be represented by sparse data, especially those for emerging materials and properties that are challenging to test, or an estimated/representative value based on manufacturer data

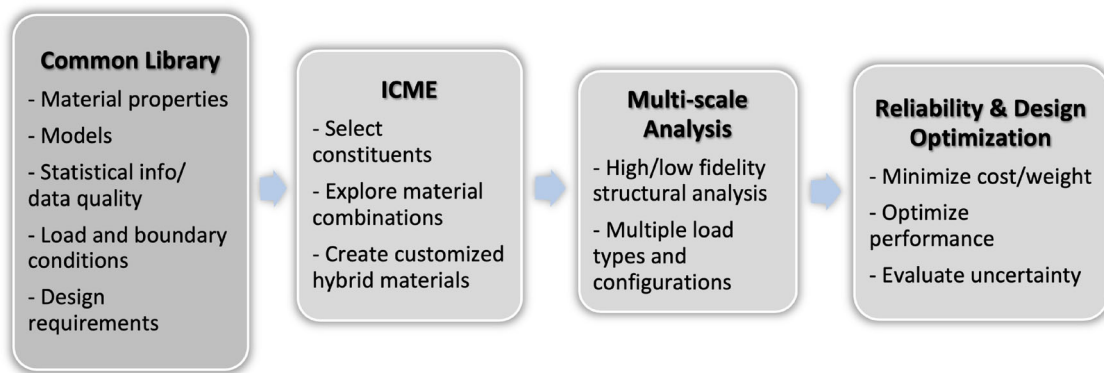


Figure 1. A simulation framework for ICME-based structural design and analysis.

sheets or experience with similar materials. Information regarding variability is often not available.

Considering the large number of property datasets required for “plug-and-play” material exploration, compounded by the need to collect data from varying sources to populate these datasets, it is essential to limit constituent material characterization to the most influential parameters and to quantify the effects of uncertain parameter data (both aleatoric and epistemic) on material properties. To address these issues, the main objectives of this study are to (1) present a method to explore the effects of data quality and sparse data on the uncertainty of mechanical properties predicted by numerical micromechanical models; and (2) enable dimension reduction using a systematic approach that limits the parameter space for uncertainty quantification (UQ) and informs focused experimental characterization on the most influential constituent parameters. These research objectives will be demonstrated through the prediction of the out-of-plane properties for a unidirectional lamina based on fiber and matrix data.

Unidirectional composites have widespread use due to their high strength-to-weight ratio. Thanks to their versatility in shape/configuration and constituents, their design is readily customized using ICME to tailor properties for specific in-situ loading conditions. While the determination of in-plane lamina properties is well documented using both analytical and computational approaches and is straightforward through experimental testing, out-of-plane lamina properties are more challenging to measure experimentally [7–12] and out-of-plane fiber properties, an input into models, are even more so [10, 13, 14]. While sophisticated measuring techniques, such as laser-based technology coupled with high fidelity modeling methods, now overcome many constraints of traditional methods [15–17], lack of data on out-of-plane properties remains a primary limitation in predicting lamina behavior. This lack of data leads to approximations resulting in unknown levels of uncertainty in predicted properties [18]. Given that data sets describing constituent properties are generally not adequate to assign probability distributions [11, 19–22], engineering judgement is often required. For example, it is common to assume that the lamina out-of-plane Poisson’s ratio  $\nu_{23}$  is equal to its in-plane counterpart  $\nu_{12}$  [23], and out-of-plane fiber properties are often indirectly calculated using micromechanics

relationships [12]. The error introduced in structural analysis results due to the use of these estimated out-of-plane properties is not well understood and may be dependent on the specific loading conditions, particularly out-of-plane loading and through-thickness stresses at discontinuities such as joints or holes. Out-of-plane properties may substantially influence the structural performance of composite laminate parts, particularly at locations of indirect stresses at corner radii, thickness changes, panel buckling, irregular load paths, and direct pressure loading [8, 24–27]. Therefore, investigation of the constitutive material parameter space and the effects of sparse data on out-of-plane lamina property prediction serve as an important example to demonstrate the developed probabilistic approach.

UQ is playing an increasingly principal role in evaluating and predicting the performance of material properties. UQ includes the quantification and propagation of uncertainties that are caused by stochastic variations in material properties, as well as uncertainties resulting from lack of data or knowledge. Many sources investigating the simulated prediction of engineering properties based on stochastic microstructure topology are available in the literature [28–34], in addition to those that address the effects of nondeterministic constitutive properties on lamina properties [35–41]. Most of these works assume a standard distribution type, such as normal or Weibull, for constitutive properties, and UQ is performed through Monte Carlo simulation [42–45]. Other methods include using fuzzy sets to model uncertain parameters [41], selective averaging method [37], Kriging-based approximation [46], and polynomial chaos expansion methods [38]. Reviews of probabilistic methods for composites are provided by Sutherland and Guedes Soares [47], Sriramula and Chryssanthopoulos [20], Shaw et al. [18], and Chamis [48]. All authors agree that constituent data is rarely fully populated, and a systematic approach to limit the parameter space to the most influential constituent properties for material characterization and to evaluate the uncertainty due to sparse data is essential to effectively predict composite properties with high confidence.

UQ using the Monte Carlo method is computationally intensive, and dimension reduction of the parameter space using global sensitivity analysis (GSA) has proven to be an effective approach to characterize the impact of uncertain model parameters on system behavior [49, 50]. Using the

results of GSA to identify the most influential parameters and limit UQ to these parameters, rather than sampling throughout the total parameter space, can reduce computation time and improve the accuracy of the uncertainty analysis. GSA further enables focused experimental data collection on these parameters that subsequently reduces the variability and uncertainty caused by lack of data. Other researchers have applied GSA in their investigation of fiber-reinforced composites, including a variance-based method [51] and global importance measures [26, 27]. We expand on prior research with a focus on investigating the effects of sparse data sets in the context of imprecise probabilities that specifically result from a lack of statistical data. The proposed method builds on the previous work of Zhang and Shields [52] who developed Bayesian multimodel and importance sampling approaches to quantify and efficiently propagate uncertainties resulting from limited data. Using this method, a set of candidate probability models are identified to represent the random constituent input that are then propagated to the prediction of out-of-plane lamina properties through finite element (FE) analysis using a representative volume element (RVE) model. To reduce the computational cost, this paper extends the imprecise GSA (IGSA) algorithm developed in [53] to consider both total-order and first-order Sobol indices so that the interaction effects between the parameters can be captured. After characterizing the relatively important parameters using extended IGSA, we focus on the variability of these important parameters instead of the overall parameter space and compare the performance of the dimension-reduced model with the original full-dimensional model.

This paper is structured as follows. Section 2 presents a brief overview of lamina property prediction using an RVE model with finite element analysis. Section 3 presents the probabilistic modeling and prediction framework using Bayesian approaches and importance sampling. A dimensionality reduction using the IGSA method, proposed in Section 4, aims to identify the critical parameters and parameter interactions in a probabilistic unidirectional composite lamina model. Section 5 summarizes the algorithm for the probabilistic framework from start to end. Section 6 applies this proposed approach to probabilistically predicting the out-of-plane unidirectional lamina properties. Finally, some concluding remarks are given in Section 7.

## 2. Deterministic prediction of unidirectional composite lamina properties

A unidirectional lamina consists of two components: the reinforcement and the matrix. When the matrix is an isotropic material and the fibers are an isotropic or transversely isotropic material, the lamina can reasonably be modeled as transversely isotropic; that is the effective properties of the lamina in the 2 and 3 (transverse, see Figure 2) plane are the same in all directions in this plane. Figure 2 demonstrates transverse isotropic behavior with the 2-3 plane (normal to the fiber direction) as the isotropic plane.

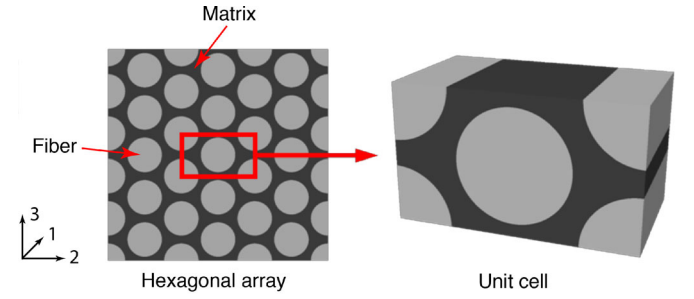


Figure 2. Hexagonal unit cell in unidirectional composite.

The overall mechanical properties of transversely isotropic unidirectional fiber-reinforced lamina are defined by five independent engineering constants which are given by the following compliance matrix:

$$C = \begin{bmatrix} 1/E_{11} & -\nu_{12}/E_{11} & -\nu_{12}/E_{11} & 0 & 0 & 0 \\ -\nu_{12}/E_{11} & 1/E_{22} & -\nu_{23}/E_{22} & 0 & 0 & 0 \\ -\nu_{12}/E_{11} & -\nu_{23}/E_{22} & 1/E_{22} & 0 & 0 & 0 \\ 0 & 0 & 0 & 1/G_{23} & 0 & 0 \\ 0 & 0 & 0 & 0 & 1/G_{12} & 0 \\ 0 & 0 & 0 & 0 & 0 & 1/G_{12} \end{bmatrix} \quad (1)$$

where  $E_{11}$  and  $E_{22}$  are the longitudinal and transverse Young's moduli, respectively,  $G_{12}$  and  $G_{23}$  are the longitudinal and transverse shear moduli,  $\nu_{12}$  is the major Poisson's ratio and  $\nu_{23}$  is the minor Poisson's ratio. The transverse shear modulus is determined from the transverse Young's modulus and minor Poisson's ratio [54] as

$$G_{23} = \frac{E_{22}}{2(1 + \nu_{23})} \quad (2)$$

Given the dependency of  $G_{23}$  on  $E_{22}$  and  $\nu_{23}$ , the focus of this study is on uncertainty in the prediction of the out-of-plane properties,  $E_{22}$  and  $\nu_{23}$ , due to sparse data characterizing the fiber and matrix material properties. For an isotropic matrix material and a transversely isotropic fiber material, eight independent constitutive properties are required to predict lamina properties using a micromechanics approach: two elastic properties describing the matrix ( $E_m$  and  $\nu_m$ ), five elastic properties describing the fiber ( $E_{1f}$ ,  $E_{2f}$ ,  $G_{12f}$ ,  $\nu_{23f}$ ,  $\nu_{12f}$ ) and one geometric property, the fiber volume fraction ( $V_f$ ).

### 2.1. RVE FE analysis

In fibrous composite analysis, homogenized properties are often obtained from microscale material sections, such as RVEs or unit cells, the smallest volume capable of representing the material as a whole. FE analysis using an RVE is a common approach for predicting the mechanical properties of a fiber-reinforced composite lamina [55–62]. The RVE allows for the relation between the constituents (fiber and matrix) and lamina-level properties to be modeled with both high fidelity and computational efficiency. RVE models provide the flexibility to rapidly investigate variation in both geometric and material properties, as well as to capture complex phenomena including the fiber-matrix interface,



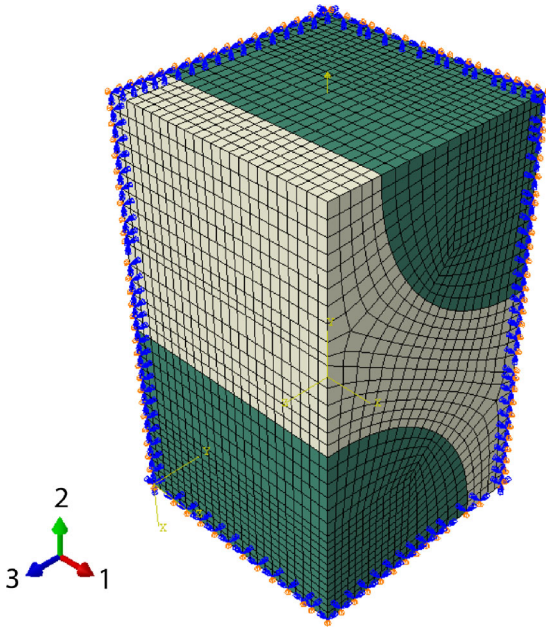


Figure 3 Hexagonal unit cell FE model.

voids and inclusions, and fiber distribution density. In this study, the material properties of the fiber and matrix and the fiber volume fraction are varied to isolate the investigation on the effects of sparse constituent property data. A perfect bond is modeled at the fiber and matrix interface. An overview of RVE modeling is provided by Li [63] and Pindera et al. [64].

Although the distribution of fibers within a composite lamina is random throughout the cross section, micromechanical unit cell RVE models simplify the micro-geometry by assuming a perfectly periodic fiber arrangement. As demonstrated in the literature (for example [9]), out-of-plane properties are sensitive to the choice of arrays for certain materials, and the hexagonal packing arrangement shown in Figure 2 has been demonstrated as the most appropriate for transversely isotropic materials [54]. For numerical simulation, periodic boundary conditions are applied to the surfaces of the RVE to force it to behave as part of a larger composite lamina, or in other words, to enforce compatible (periodic) behavior. Application of periodic boundary conditions in multi-phase materials is a topic that has been studied in great detail [65–68] and therefore will not be further discussed here. The RVE model is established as a three-dimensional RVE with two symmetry planes in the 1-3 and 1-2 directions, and the aforementioned periodic boundary conditions as illustrated in Figure 3. The mesh for this model consists of 20448 C3D8R solid elements and 22750 nodes and was analyzed in Abaqus Standard.

While FE analysis provides a computationally efficient method to rapidly analyze an RVE, it is more user-intensive to set up and computationally demanding to solve than closed-form, empirical micromechanical equation-based methods due to the large number of model evaluations required for GSA. To address this challenge, an automated mesh generation script was created, which provides quality

control through element size requirements. This automation alleviates user-intensive tasks associated with generating discretized RVE microstructures for successive simulations and extracting and compiling output data after each analysis. This tool enables the user to obtain homogenized lamina properties through a single initiation allowing for automated GSA and UQ studies.

## 2.2. Calculation of out of plane lamina properties

Out-of-plane lamina properties were calculated from the FE results using a homogenization approach based on energy principles and Gauss's Theorem, as detailed by Sun and Vaidya [9]. Given a macroscopically homogenous medium with boundary tractions that produce uniform stresses and strains, equilibrium conditions and Gauss's Theorem are applied to prove that the strain energy stored in the effective homogenous medium ( $U$ ) equals that of a heterogeneous medium ( $U'$ ) provided that the same boundary tractions are applied and perfect bonding occurs between constituents. The boundary conditions force the average displacement ( $\bar{u}_i$ ) and displacement at any location on the surface ( $u_i$ ) to be equal. That is,

$$U - U' = \frac{1}{2} \int_V \sigma_{ij} \left( \frac{\partial u_i}{\partial x_j} - \frac{\bar{u}_i}{\partial x_j} \right) dV = \frac{1}{2} \int_S \sigma_{ij} (u_i - \bar{u}_i) n_j dS = 0 \quad (3)$$

The average strain in a two-phase material is derived through Gauss's Theorem. The composite cross section is assumed to be perfectly periodic such that a single RVE can be used to replicate the internal and repeating stress and strain gradients that arise under uniform loading conditions. When acted upon by a uniform load, the homogenized strain field within the RVE can be determined from the boundary displacements using Gauss's Theorem, a means of relating the flow of a vector field through a surface to the internal behavior of the vector field [69]. Gauss's Theorem converts the volume integral used to obtain the average strain into three simple surface integrals that occur over the outer fiber boundary ( $-S_1$ ), inner matrix boundary ( $S_1$ ), and outer matrix boundary ( $S_2$ ). The surface integration at the fiber-matrix interface is posed to occur in opposite directions, which reverses one of the signs and causes the integrals to cancel out. Therefore, the average strain can be evaluated using the remaining surface integral which only consists of the external surface displacements and their associated normals:

$$\bar{\epsilon}_{ij} = \frac{1}{2V} \int_{S_2} (u_i n_j + u_j n_i) dS \quad (4)$$

Because the periodic boundary conditions force the cell boundaries to displace in a controlled and known manner, only a single boundary displacement from each surface, determined from FEA, is needed to calculate the average volumetric strain ( $\bar{\epsilon}_{ij}$ ). This approach is favorable because extracting and using the surface displacements is more computationally efficient than extracting and averaging the strain

in every element. The average strain in the principal directions can then be used to calculate the homogenized (averaged) properties using Hooke's law.

In the finite element model of the RVE, a transverse tension load is applied as a uniform stress ( $P_2$ ) acting along the 2-axis (Figure 3), and  $u_2$  and  $u_3$  are the resulting surface displacements along the 2-axis and 3-axis respectively. Surfaces are assumed to remain planar during normal loading to enforce compatible behavior of the unit cell. The average strain due to the normal tensile stress is formulated as:

$$\bar{\epsilon}_{22} = \frac{u_2}{l_2} \quad (5)$$

where  $l_2$  is the length of the RVE in the 2 direction. Substituting this average strain into the strain energy equation and equating it to the work done on the RVE ( $W$ ) enables calculation of the average stress as

$$U = W \quad \text{or} \quad \frac{1}{2} \bar{\sigma}_{22} \bar{\epsilon}_{22} V = \frac{1}{2} P_2 \cdot l_1 \cdot l_3 \cdot u_2. \quad (6)$$

Subsequently, the effective transverse modulus ( $E_2$ ) and Poisson's ratio ( $\nu_{23}$ ) are calculated as

$$E_2 = \frac{P_2 \cdot l_2}{u_2} \quad \text{and} \quad \nu_{23} = -\frac{u_3}{u_2} \quad (7)$$

for the case where all lengths of the RVE are equal.

### 3. Bayesian multimodel UQ method

Typically, probabilistic modeling requires either assumptions (e.g. knowledge from experience or expert opinion) or large data sets to characterize probability distributions. Often in engineering practice, however, only limited data are available so that it is difficult to assign an accurate probability distribution. This section presents a review of the Bayesian multimodel framework proposed previously by the authors [52, 70], where the uncertainties resulting from small data sets are quantified and efficiently propagated using importance sampling reweighting.

#### 3.1. Bayesian multimodel framework

The uncertainties resulting from small material property data sets consist of model-form uncertainty and model parameter uncertainty. That is, we are not unsure what distribution family (model) best represents the data, nor are we sure of the precise parameter values for that distribution. The problem of probability model selection considers identifying a model  $M_i$  that best represents the data  $\mathbf{d}_p$  given a set of  $N_p$  candidate probability models  $\mathcal{M} = \{M_j\}, j = 1, \dots, N_p$ . However, when data are sparse it is not possible to determine a single "best" model for the data. In this work, we apply Bayesian multimodel inference, as introduced by Burnham and Anderson [71], to estimate the model uncertainty by identifying multiple candidate models and their associated model probabilities.

In the Bayesian multimodel setting, model prior probabilities  $\pi_j = p(M_j)$  with  $\sum_{j=1}^{N_p} \pi_j = 1$  are assigned to each model in  $\mathcal{M}$ . According to Bayes' rule, we can estimate the

posterior model probabilities given the data  $\mathbf{d}_p$  as follows:

$$\hat{\pi}_j = p(M_j|\mathbf{d}_p) = \frac{p(\mathbf{d}_p|M_j)p(M_j)}{\sum_{j=1}^{N_p} p(\mathbf{d}_p|M_j)p(M_j)}, \quad j = 1, \dots, N_p \quad (8)$$

having  $\sum_{j=1}^{N_p} \hat{\pi}_j = 1$ , where the evidence of model  $M_j$  is given by:

$$p(\mathbf{d}_p|M_j) = \int_{\theta_j} p(\mathbf{d}_p|\theta_j, M_j)p(\theta_j|M_j)d\theta_j, \quad j = 1, \dots, N_p \quad (9)$$

Notice that the evidence plays an essential role in Bayesian multimodel inference, as evident from Eq.(8). A detailed discussion of the evidence calculation can be found in [70]. Unlike conventional model selection, where the model  $M_k \in \mathcal{M}$  with the highest posterior probability  $p(M_k|\mathbf{d}_p)$  is selected as the "best" model, Bayesian multimodel inference ranks the candidate model based on their posterior model probabilities and retains all plausible models with nonnegligible probabilities [52].

Once the candidate model sets and their associated posterior model probabilities have been determined, additional uncertainties associated with the model parameters also need to be taken into account given limited data. For each candidate model  $M_j, j = 1, \dots, m$ , the parameter uncertainty can be quantified via Bayesian inference. Using Bayes' rule, we estimate the posterior parameter distribution by:

$$p(\theta_j|\mathbf{d}_p, M_j) = \frac{p(\mathbf{d}_p|\theta_j, M_j)p(\theta_j|M_j)}{p(\mathbf{d}_p|M_j)}, \quad j = 1, \dots, m \quad (10)$$

where  $p(\mathbf{d}_p|\theta_j, M_j)$  is the likelihood function and  $p(\theta_j|M_j)$  is the parameter prior pdf. Markov Chain Monte Carlo (MCMC) sampling is used here to estimate the posterior distribution. Typically, Bayesian inference is used to identify a unique posterior parameter vector  $\theta_j$  as a point estimator, such as the maximum a posterior estimator (MAP) or maximum likelihood estimate (MLE). Yet, in the limited data case, the posterior distributions will likely possess large variance and a point estimator neglects the distribution parameter uncertainties. For this reason, we retain the full posterior probability density  $p(\theta_j|\mathbf{d}_p, M_j)$  for each model,  $M_j$  as a measure of parameter uncertainty.

The process of Bayesian multimodel inference theoretically yields an infinite set of probability distributions [52]. In practice, we need to reduce this to a finite, but statistically representative, set of  $N_r$  probability distributions. This can be achieved by random sampling from the infinite set of probability distributions. For each distribution, we randomly select a model  $M_i \in \mathcal{M}$  with model probability  $\hat{\pi}_i = p(M_i|\mathbf{d}_p)$  and randomly select its parameters from the joint posterior parameter density  $p(\theta_i|\mathbf{d}_p, M_i)$ . Note that  $N_r$  can be chosen arbitrarily large to fully characterize the uncertainties caused by the lack of data without adding appreciable computational cost to the analysis. The interested reader can find more details and discussions in [52].

### 3.2. Uncertainty propagation using importance sampling

Importance sampling is a variance reduction technique applied to estimate a statistical expectation with respect to a target probability distribution  $p(\mathbf{x})$  using samples drawn from an alternative distribution  $q(\mathbf{x})$ . Specifically, the expected value  $\mu = E_p[f(\mathbf{x})]$  with respect to  $p(\mathbf{x})$  is formulated by

$$\begin{aligned}\mu &= E_p[f(\mathbf{x})] = \int f(\mathbf{x})p(\mathbf{x})d\mathbf{x} = \int \frac{f(\mathbf{x})p(\mathbf{x})}{q(\mathbf{x})}q(\mathbf{x})d\mathbf{x} \\ &= E_q\left[\frac{f(\mathbf{x})p(\mathbf{x})}{q(\mathbf{x})}\right]\end{aligned}\quad (11)$$

where  $E_q[\cdot]$  denotes expectation with respect to  $q(\mathbf{x})$ . Defining importance weights  $w(\mathbf{x}) = p(\mathbf{x})/q(\mathbf{x})$ , the importance sampling estimator of  $E_p[f(\mathbf{x})]$  is

$$\hat{\mu}_p = E_p[f(\mathbf{X})] \approx \frac{1}{N} \sum_{i=1}^N \frac{f(\mathbf{x}_i)p(\mathbf{x}_i)}{q(\mathbf{x}_i)} = \frac{1}{N} \sum_{i=1}^N f(\mathbf{x}_i)w(\mathbf{x}_i) \quad (12)$$

The variance of the importance weights and the closely related effective sample size [72] provide useful measures to determine the quality of an importance sampling estimator. Interested readers can find a related study on the effectiveness of importance sampling reweighting in [73].

In the multimodel setting, we have an ensemble of target plausible models  $p_i(\mathbf{x})$  and the challenge then is how to identify a single sampling density  $q(\mathbf{x})$  that is optimally representative of all target densities. Zhang and Shields [52] address this issue by providing an explicit analytical derivation for the optimal importance sampling density given all candidate target densities. This method uses the mean square difference (MSD) to calculate the difference between one target density and one importance sampling density, which is given by

$$\mathcal{M}(P \parallel Q) = \frac{1}{2} \int (p(\mathbf{x}|\boldsymbol{\theta}) - q(\mathbf{x}))^2 d\mathbf{x} \quad (13)$$

The total expected mean-squared difference between the ensemble of  $N_p$  probability models  $p_j(\mathbf{x}|\boldsymbol{\theta}_j), j = 1, \dots, N_p$  and a single importance sampling density  $q(\mathbf{x})$  can be expressed as follows:

$$\mathcal{E} = \sum_{j=1}^{N_p} E[\mathcal{M}(P_j \parallel Q)] = E_{\theta} \left[ \int \sum_{j=1}^{N_p} \frac{1}{2} (p_j(\mathbf{x}|\boldsymbol{\theta}_j) - q(\mathbf{x}))^2 d\mathbf{x} \right] \quad (14)$$

The following constrained optimization problem is then solved to minimize the total expected mean-squared difference expressed as a functional  $\mathcal{L}(q)$  under isoperimetric constraint  $\mathcal{I}(q)$ :

$$\begin{aligned}\text{minimize}_q \quad & \mathcal{L}(q) = E_{\theta} \left[ \int \mathcal{F}(\mathbf{x}, \boldsymbol{\theta}, q(\mathbf{x})) d\mathbf{x} \right] \\ \text{subject to} \quad & \mathcal{I}(q) = \int q(\mathbf{x}) d\mathbf{x} - 1 = 0\end{aligned}\quad (15)$$

where the action functional  $\mathcal{F}(\cdot)$  is the total square differences:

$$\mathcal{F}(\mathbf{x}, \boldsymbol{\theta}, q(\mathbf{x})) = \frac{1}{2} \sum_{j=1}^{N_p} (p_j(\mathbf{x}|\boldsymbol{\theta}_j) - q(\mathbf{x}))^2 \quad (16)$$

and  $E_{\theta}$  is the expectation with respect to the posterior probability density of the model parameters  $\boldsymbol{\theta}$ . The constraint  $\mathcal{I}(q)$  ensures that  $q(\mathbf{x})$  is a valid probability density function. Notice that the optimization problem in Eq. (15) has a closed-form solution given by the convex mixture model [52]

$$q^*(\mathbf{x}) = \frac{1}{N_p} \sum_{j=1}^{N_p} E_{\theta} [p_j(\mathbf{x}|\boldsymbol{\theta}_j)] \quad (17)$$

and this solution can be generalized to include the posterior model probabilities as

$$q^*(\mathbf{x}) = \sum_{j=1}^{N_p} \hat{\pi}_j E_{\theta} [p_j(\mathbf{x}|\boldsymbol{\theta}_j)] \quad (18)$$

where  $\hat{\pi}_j$  is the posterior model probability for model  $M_j$ , computed by Eq. (8). In the multivariate case, if each random variable is independent, the optimal sampling density can be identified for each random variable independently and then multiplied to obtain the joint optimal sampling density.

For uncertainty propagation, samples are drawn from the optimal sampling density  $q^*(\mathbf{x})$  and the response of the model  $f(\mathbf{x})$  is evaluated at each sample point. The quantity of interest is then reweighted according to each of the  $N_r$  sample pdfs according to the importance weights.

## 4. Dimensionality reduction with global sensitivity analysis

Sensitivity analysis is a widely used approach to quantitatively assess the influence of variations in input variables on the output quantity of interest (QoI). It therefore allows us to assess the relative importance of each model input to the specific QoI. In accordance with the sensitivity index for each variable, we can then reduce the model dimensionality by focusing on the relatively important variables. This section briefly outlines that process when sensitivity indices are estimated from small data sets.

### 4.1. Variance-based sensitivity analysis

Variance-based sensitivity analysis decomposes the variance of the output of the model or system into fractions that can be attributed to each input parameter. A specific measure of variance-based sensitivity that is commonly used is the so-called Sobol indices [74] that are defined as the relative contribution of the partial variances  $V_{i_1, \dots, i_s}$  to the total variance  $V$

$$S_{i_1, \dots, i_s} = \frac{V_{i_1, \dots, i_s}}{V} = \frac{V_{i_1, \dots, i_s}}{\sum_{i=1}^d V_i + \sum_{1 \leq i < j \leq d} V_{ij} + \dots + V_{1, 2, \dots, d}} \quad (19)$$

such that:

$$\sum_{i=1}^d S_i + \sum_{1 \leq i < j \leq d} S_{ij} + \dots + S_{1,2,\dots,d} = 1 \quad (20)$$

where  $S_i$  is commonly referred to as the *first-order* index that measures the contribution of each input variable  $x_i$  to the variance of model output  $y$  taken separately without interacting with any other inputs.  $S_{ij}$  is the *second-order* index which estimates the contribution of interactions between variable  $x_i$  and  $x_j$  to the total variance. One can infer the impact of each input variable and the interaction of variables on the output variance using  $S_i$ ,  $S_{ij}$  and high-order indices in Eq. (20). Another popular variance based measure known as the *total-order* index is typically used to estimate the contribution of variable  $x_i$  and its interactions to the output variance. It is given as follows:

$$S_i^T = \sum_{\{i\} \subset \{i_1, \dots, i_s\}} \frac{V_{i_1, \dots, i_s}}{V} \quad (21)$$

Note that unlike the  $S_i$ ,

$$\sum_{i=1}^d S_i^T \geq 1 \quad (22)$$

This is because the interaction between  $x_i$  and  $x_j$  is counted in both  $S_i^T$  and  $S_j^T$ . The sum of the  $S_i^T$  is equal to 1 if and only if the model is purely additive without any interaction effects.

The first-order indices  $S_i$  in Eq. (20) and total-order indices  $S_i^T$  in Eq. (21) can be calculated as follows:

$$S_i = \frac{V_i}{V} = \frac{\text{Var}_{x_i}[E_{x_{-i}}[y|\mathbf{x}_i]]}{\text{Var}[y]} \quad (23)$$

$$S_i^T = \sum_{\{i\} \subset \{i_1, \dots, i_s\}} \frac{V_{i_1, \dots, i_s}}{V} = 1 - \frac{\text{Var}_{x_{-i}}[E_{x_i}[y|\mathbf{x}_{-i}]]}{\text{Var}[y]} \quad (24)$$

where  $\text{Var}_{x_i}[\cdot]$  denotes the variance when only  $x_i$  is allowed to vary and  $E_{x_{-i}}(\text{Var}_{x_{-i}}[\cdot])$  denotes the expectation (variance) when all variables except  $x_i$  are allowed to vary.

The calculation of the Sobol indices in Eqs. (23) and (24) analytically is not typically possible except in the case of certain simple analytical functions. Instead, Monte Carlo methods are employed to compute the Sobol indices. There are a number of possible Monte Carlo estimators available for both indices. Two that are currently in general use are proposed by Saltelli [49]

$$V_i = \text{Var}_{x_i}[E_{x_{-i}}[y|\mathbf{x}_i]] \approx \frac{1}{m} \sum_{k=1}^m f(\mathbf{x}^k) \left( f(\mathbf{x}_i^k, \xi_{-i}^k) - f(\xi^k) \right) \quad (25)$$

$$V_{i_1, \dots, i_s} = E_{x_{-i}}[\text{Var}_{x_i}[y|\mathbf{x}_{-i}]] \approx \frac{1}{2m} \sum_{k=1}^m \left( f(\xi^k) - f(\mathbf{x}_i^k, \xi_{-i}^k) \right)^2 \quad (26)$$

where  $\xi_{-i}$  denotes all the variables in  $\xi$  not including  $\xi_i$ . The subscript  $i$  is the index of the model inputs, superscript  $k$  is the index of the samples and  $m$  is the number of

samples. For the estimation of the  $S_i$  and  $S_i^T$  for all input variables, we require  $m$  samples of  $\mathbf{x}$  and  $m$  samples of  $\xi$ , both of which are independently drawn from the joint probability distribution  $p(\mathbf{x})$  of the model inputs. The overall computational cost for estimating  $S_i$  and  $S_i^T$  is  $(d+2)m$  model evaluations, where  $d$  is the dimension of the vector  $\mathbf{x}$ . Since  $m$  is often on the order of thousands, the computational cost can quickly become a challenge if a single-model evaluation is expensive. In such cases, various approaches have been recently proposed to improve the formulation of the Sobol indices with more accurate estimates, or improve the efficiency of the estimator using variance reduction approaches, for example, Latin hypercube sampling [75, 76] or surrogate models. We do not elaborate on these methods here because they are not our main priority in this study.

#### 4.2. Simultaneous estimation of multimodel Sobol indices

As discussed in Section 3, the uncertainties resulting from limited data are represented by a set of  $N_p$  probability models and their joint posterior parameter distributions  $p(\theta_j | \mathbf{d}_p, M_j)$ , which are statistically sampled for a total of  $N_r$  candidate distributions. Again, it is important to emphasize that  $N_r$  must be a sufficiently large number such that it can adequately represent the overall uncertainties in both probability model-form and parameters. If the conventional Monte Carlo method is employed to estimate the Sobol indices for each model, the total number of model evaluation is  $N_r \times (d+2) \times m$ . This leads to a prohibitively large computational cost for the estimation of multi-model Sobol indices. To overcome this challenge, an efficient imprecise global sensitivity analysis (IGSA) method has been recently proposed by the authors [53]. This method utilizes importance sampling reweighting to reduce the total cost of imprecise GSA from  $\mathcal{O}(N_p^d dm)$  to  $\mathcal{O}(N_p dm)$  and achieve simultaneous computation of first-order and total-order Sobol indices for all  $N_r$  distributions.

Considering the statistical set  $\mathcal{P}$  of target densities  $p_j(\mathbf{x}|\theta_j)$ ,  $j = 1, \dots, N_r$ , the  $i$ th partial variance in first-order Sobol indices  $S_i$  given the  $j$ th target density  $p_j(\mathbf{x}|\theta_j)$  is estimated as follows:

$$V_i^j = \int f(\mathbf{x}) p_j(\mathbf{x}|\theta_j) [f(\mathbf{x}_i, \xi_{-i}) p_j(\xi_{-i}|\theta_j) - f(\xi) p_j(\xi|\theta_j)] d\mathbf{x} d\xi \quad (27)$$

According to the importance sampling method, the partial variance in Eq. (27) can be rewritten in terms of the importance sampling density,  $q(\mathbf{x})$ , as

$$V_i^j = \int f(\mathbf{x}) \frac{p_j(\mathbf{x}|\theta)}{q(\mathbf{x})} q(\mathbf{x}) \left[ f(\mathbf{x}_i, \xi_{-i}) \frac{p_j(\xi_{-i}|\theta)}{q(\xi_{-i})} q(\xi_{-i}) - f(\xi) \frac{p_j(\xi|\theta)}{q(\xi)} q(\xi) \right] d\mathbf{x} d\xi \quad (28)$$

Hence, the estimator in Eq. (25) can be modified by importance sampling reweighting as



$$\begin{aligned}\hat{V}_i^j &\approx \frac{1}{m} \sum_{k=1}^m f(\mathbf{x}^k) \frac{p_j(\mathbf{x}^k|\boldsymbol{\theta})}{q(\mathbf{x}^k)} \left[ f(\mathbf{x}_i^k, \boldsymbol{\xi}_{-i}^k) \frac{p_j(\boldsymbol{\xi}_{-i}^k|\boldsymbol{\theta})}{q(\boldsymbol{\xi}_{-i}^k)} - f(\boldsymbol{\xi}^k) \frac{p_j(\mathbf{x}^k|\boldsymbol{\theta})}{q(\mathbf{x}^k)} \right] \\ &\approx \frac{1}{m} \sum_{k=1}^m f(\mathbf{x}^k) w_j(\mathbf{x}^k) \left[ f(\mathbf{x}_i^k, \boldsymbol{\xi}_{-i}^k) w_j(\boldsymbol{\xi}_{-i}^k) - f(\boldsymbol{\xi}^k) w_j(\mathbf{x}^k) \right]\end{aligned}\quad (29)$$

We can further generalize this approach to modify the total-order indices  $S_i^T$  in Eq. (26) using importance sampling reweighting as follows:

$$\begin{aligned}\hat{V}_{i_1, \dots, i_s}^j &\approx \frac{1}{2m} \sum_{k=1}^m \left[ f(\boldsymbol{\xi}^k) \frac{p_j(\mathbf{x}^k|\boldsymbol{\theta})}{q(\mathbf{x}^k)} - f(\mathbf{x}_i^k, \boldsymbol{\xi}_{-i}^k) \frac{p_j(\boldsymbol{\xi}_{-i}^k|\boldsymbol{\theta})}{q(\boldsymbol{\xi}_{-i}^k)} \right]^2 \\ &\approx \frac{1}{2m} \sum_{k=1}^m \left[ f(\boldsymbol{\xi}^k) w_j(\mathbf{x}^k) - f(\mathbf{x}_i^k, \boldsymbol{\xi}_{-i}^k) w_j(\boldsymbol{\xi}_{-i}^k) \right]^2\end{aligned}\quad (30)$$

Eqs. (29) and (30) allow us to estimate the Sobol indices  $S_i$  and  $S_i^T$  using only a single Monte Carlo simulation with importance sampling density  $q(\mathbf{x})$ , then reweight the importance sampling estimator for each of the  $N_r$  candidate target densities. The selection of sampling density is critical to accurately estimate the Sobol indices. For this, we employ the optimal sampling density from Eq. (18) above.

The result of applying Eqs. (29) and (30) and reweighting is a statistical set of first-order and total-order sensitivity indices. This statistical set can be used to estimate statistical quantities for the sensitivity indices include empirical cdf's and moments that can be used to quantify uncertainty in these sensitivities that arise from sparse data.

## 5. Probabilistic prediction framework

A fundamental challenge in probabilistic prediction is high-dimensional uncertainty propagation. The IGSA method allows us to quantitatively understand the relative influence of random inputs on the output QoI, including uncertainty that derives from having only limited data. Thus, more effort can be spent on the more sensitive variables (e.g. increased data collection) rather than the variables whose role is limited. As a result, the model dimension is reduced by using the variables with higher sensitivity indices. Algorithm 1 summarizes the proposed step-by-step approach for probabilistic prediction with the dimension-reduced model.

The algorithm starts with initial data collection for each model input. The Bayesian multimodel method is then used to quantify the uncertainties associated with the probability model and the corresponding model parameters. This is followed by establishing a finite probability model set to represent the imprecise probabilities caused by the lack of data. Next, the optimal sampling density is derived by solving the optimization problem and random samples are drawn from the optimal sampling density. The importance weights are calculated for each random variable and the model is evaluated at this points. According to the joint importance weights, we calculate the first-order and total-order Sobol indices by only reweighting each of the model evaluations and then evaluate the relative importance and interaction

among the random model inputs. Finally, we identify the ranked model inputs and reduce the model dimension by only focusing on the relatively important variables. The imprecise sensitivities can then inform further data collection efforts. In particular, data collection would focus on those variables that have both high uncertainty and high probability of having significant sensitivity index.

The proposed probabilistic prediction framework is easily updated to accommodate additional collected data because the importance weights can be updated directly for the new data without additional model evaluations. However, this causes a loss of optimality in the importance sampling density. This is due to changes in the set of plausible target densities characterized by Bayesian multimodel inference, as discussed in [52]. A recent study proposes an efficient Monte Carlo resampling algorithm to minimize the impact on the computational cost and sample set in Bayesian updating [73].

## 6. Application to out-of-plane unidirectional carbon fiber composites

In this work, we apply the proposed probabilistic analysis framework to explore the influence of the constituent (carbon fiber and epoxy resin) material properties on the out-of-plane elastic properties of a unidirectional composite lamina.

### 6.1. Identifying constituent material property distributions

A common type of composite lamina is one fabricated from carbon fibers and 3501-6 epoxy resin matrix. An extensive literature search for the material properties of AS4 carbon revealed that published experimental test data for out-of-plane properties is limited and inconsistent, although this material is widely used. The data were found to be inconsistent or recycled amongst sources, particularly for the out-of-plane properties of the AS4 carbon fibers, and the origin of the data was not always stated. The sparseness and questionable validity of this constituent data (Tables 1 and 2) makes AS4/3501-6 an exemplary material to be evaluated through IGSA using Bayesian multimodel inference to identify the model input distributions.

These collected data are classified as extremely sparse. For such sparse data, Bayesian uncertainty quantification begins by assigning priors to each material parameter. According to the literature review and authors' experience, a uniform prior with upper and lower bounds are provided for the mean and coefficient of variation (COV) of each material property, as shown in Table 3.

In the context of Bayesian multimodel inference, we select five typical candidate probability models, i.e. Gamma, Inverse Gaussian, Logistic, Lognormal and Normal. With equal prior model probabilities  $\pi_j = 0.2, j = 1, \dots, 5$  for each model, we can calculate the posterior model probabilities  $\hat{\pi}_j, j = 1, \dots, 5$ , which are shown in Table 4. Notice that the sparse data plays a very limited role in the posterior model probabilities, which remain largely unchanged. In other

**Table 1.** 3501-6 epoxy resin matrix material properties from literature.

Source	$E_m$ (GPa)	$\nu_m$
Soden [77]	4.2	0.34
Karami and Garnich [78]	4.3	0.35
Yim and Gillespie [79]	4.3	0.34
Blacketter et al. [80]	4.4	0.34
Adams and Adams [81]	4.2	/
Guagliano and Riva [82]	4.4	0.34
Nicoletto and Riva [83]	4.8	0.34
Hexcel data sheet [84]	4.2	/
Daniel and Ishai [85]	4.3	0.35

words, it is impossible to identify a unique probability model for these material parameters from the given data.

Once the model-form uncertainty is quantified, we then estimate the posterior joint density of model parameters using Bayesian inference with MCMC sampling. Next, a finite set of probability models is established by combining the model-form and model parameter uncertainties. Figure 4 shows the ensemble of candidate target probability distributions for each material property. The gray curves represent the cloud of 500 candidate distributions and the thick black curve represents the optimal sampling density, which is determined by solving the constrained optimization discussed above. It can be observed that the variables with extremely sparse data ( $\nu_{23f}$ ,  $\nu_m$ ,  $V_f$  and  $G_{12f}$ ) have a wider distribution cloud but the distributions  $E_m$ ,  $\nu_m$ , and  $E_{1f}$  are narrower as expected because they have more data.

## 6.2. Assessing the impact of constituent properties on out-of-plane composite properties

In the Bayesian multimodel framework, 500 candidate target densities have been identified for each material property. For such cases, there are an immense number ( $500^8 \approx 4^{21}$ ) of total combinations of these distributions. Even though the reweighting approach proposed herein does not require model evaluations, this significant number is still prohibitive. Instead, we select a representative 5000 joint target distributions that are compiled using Latin hypercube sampling. To estimate the first-order and total-order Sobol indices, we draw 50,000 random samples from the optimal sampling density of each material property and then reweight these samples according to the imprecise GSA algorithm. The computational model evaluations are performed using FEM for the RVE introduced in Section 2.

In this study, we are interested in two composite elastic properties: Elastic modulus along the 2 direction,  $E_2$ , and the Poisson's ratio in the 2-3 direction,  $\nu_{23}$ . Figure 5 shows histograms of the first-order (blue color) and total-order (orange color) Sobol indices for  $E_2$ . Note that the distribution of first-order and total-order Sobol indices are nearly identical, meaning there are no significant interactions among these input parameters. We can, therefore, identify the relatively important variables through the first-order Sobol indices alone. As for  $E_2$ , it can be observed, even with very limited data, that the volume fraction  $V_f$  has a very high probability of being the most significant property, but due to the lack of data the sensitivity of  $V_f$  exhibits a noteworthy variation ranging from approximately 0.2 to 0.8. The

**Table 2.** Carbon fiber material properties from literature.

Source	$E_{1f}$ (GPa)	$E_{2f}$ (GPa)	$G_{12f}$ (GPa)	$\nu_{12f}$	$\nu_{23f}$
ASM Engineering Materials [86]	234	14	/	/	/
Unknown	234.95	13.78	27.97	0.2	/
Daniel and Ishai [85]	235	15	27	0.2	/
King et al. [10]	235	14	28	0.2	0.25
Handbook of Materials Selection [87]	235	/	/	/	/
Composites Engineering Handbook [88]	235	/	/	/	/
Yim and Gillespie [79]	235	14	28	0.2	/

second most significant variable is likely the matrix Elastic modulus  $E_m$ , which has a mean Sobol index of 0.31 and ranges from 0.1 to 0.7, although there are cases where  $E_m$  is the most influential property. The fiber Elastic modulus along the 2 direction  $E_{2f}$ , with a mean Sobol index of 0.24 and a range from 0.07 to 0.5, also shows a moderate-to-high impact on  $E_2$ . The other five material properties play nearly no role in determining  $E_2$ . As a result, we ranked these material properties according to their relative importance, which is quantified by the mean of the first-order Sobol indices, and finally identify the top 3 important material properties for  $E_2$  as: 1.  $V_f$ , 2.  $E_m$ , and 3.  $E_{2f}$ . This simple measure of importance was sufficient for our purposes, but because the approach yields distributions of Sobol indices, one could consider more advanced metrics such as estimating the probability that a given parameter has the highest Sobol index.

Figure 6 shows histograms of the first-order and total-order Sobol indices for  $\nu_{23}$ . In this case, the volume fraction  $V_f$  is still important but is not the most significant variable. Instead, the matrix Poisson's ratio  $\nu_m$  becomes the most significant variable with first-order Sobol indices ranging from approximately 0.4 to 0.95. Another important variable is the fiber Poisson's ratio along 2-3 direction  $\nu_{23f}$ , which shows a range from 0 to 0.3. Even with such a small dataset, we can observe that the other five variables,  $\nu_{12f}$ ,  $E_m$ ,  $E_{1f}$ ,  $E_{2f}$ , and  $G_{12f}$  have such a little influence that their impact on  $\nu_{23}$  can be effectively ignored. Again, there are no strong interaction effects demonstrated between the parameters used to calculate  $\nu_{23}$ , as we see by comparing the histogram of first-order and total-order Sobol indices. Consequently, we identify that the first three important variables are  $\nu_m$ ,  $V_f$  and  $\nu_{23f}$  based on the mean of their first-order Sobol indices.

## 6.3. Probabilistic prediction of composite out-of-plane elastic properties

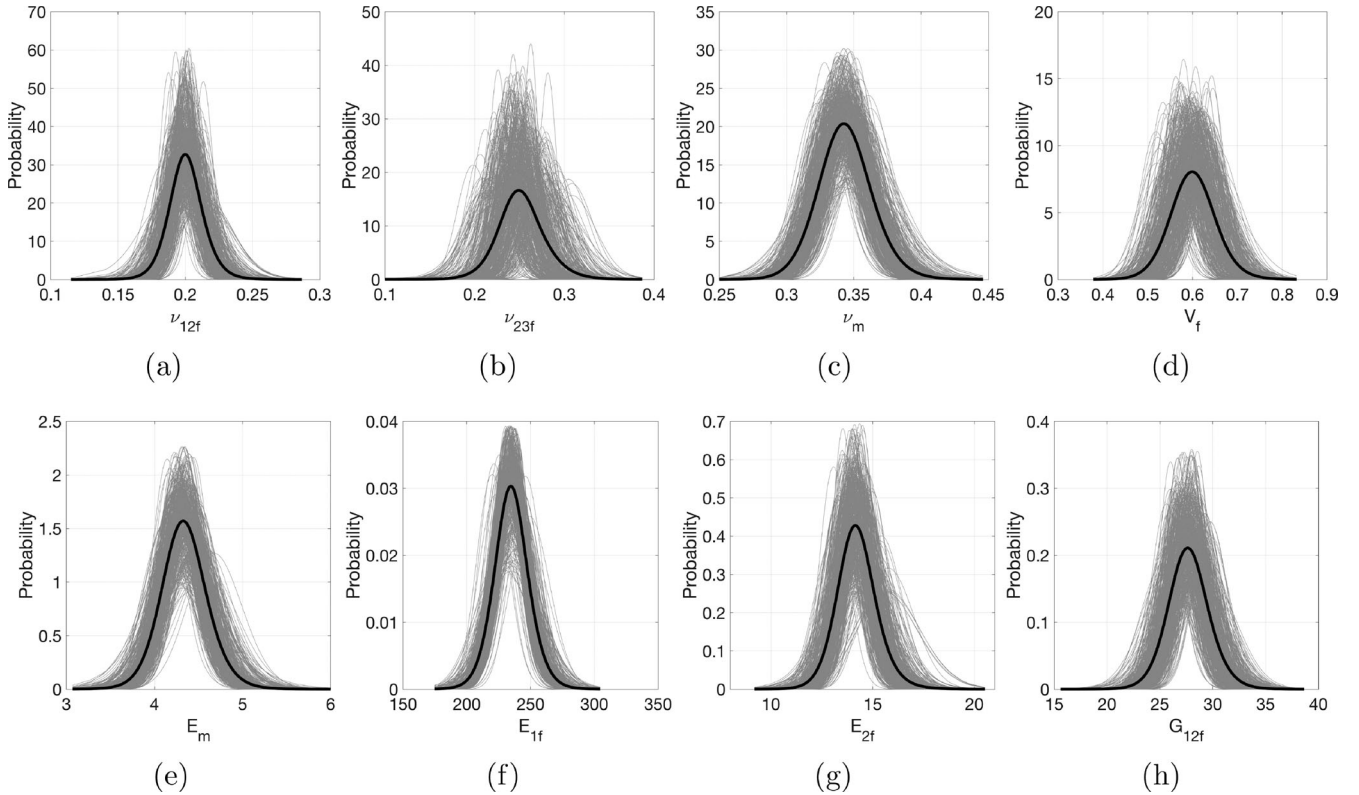
Using the IGSA approach, we identified the most important variables according to their first-order Sobol indices. Variation in the other variables with minor impact can be effectively ignored in probabilistic modeling. This provides a potential for dimension reduction of the computational model. As for the carbon fiber composite application considered here, the total eight random variables can be reduced to three important variables which were identified from IGSA. In the meantime, the variation from the other five variables is ignored and they are represented by their statistical mean value. Here, we are specifically interested in

**Table 3.** AS4 Carbon fiber/3501-6 Epoxy Resin composite material model.

Material Property	Physical meaning	Number of data	Mean bound	COV bound
$\nu_{12f}$	Fiber Poisson's ratio along 1-2 direction	4	[0.15, 0.25]	[5%, 10%]
$\nu_{23f}$	Fiber Poisson's ratio along 2-3 direction	1	[0.2, 0.3]	[5%, 10%]
$\nu_m$	Matrix Poisson's ratio	7	[0.3, 0.4]	[5%, 10%]
$V_f$	Fiber volume fraction	1	[0.55, 0.65]	[5%, 10%]
$E_m$ (GPa)	Matrix Young's modules	9	[4, 5]	[5%, 10%]
$E_{1f}$ (GPa)	Fiber Young's modules along 1 direction	7	[200, 250]	[5%, 10%]
$E_{2f}$ (GPa)	Fiber Young's modules along 2 direction	5	[10, 20]	[5%, 10%]
$G_{12f}$ (GPa)	Fiber shear modules along 1-2 direction	4	[25, 30]	[5%, 10%]

**Table 4.** Model probabilities from the given data for each material property.

Distribution	$\hat{\pi}_{\nu_{12f}}$	$\hat{\pi}_{\nu_{23f}}$	$\hat{\pi}_{\nu_m}$	$\hat{\pi}_{V_f}$	$\hat{\pi}_{E_m}$	$\hat{\pi}_{E_{1f}}$	$\hat{\pi}_{E_{2f}}$	$\hat{\pi}_{G_{12f}}$
Normal	0.200	0.200	0.197	0.200	0.137	0.143	0.176	0.195
Lognormal	0.200	0.200	0.206	0.200	0.186	0.142	0.195	0.188
Gamma	0.200	0.200	0.211	0.200	0.173	0.148	0.200	0.205
Inverse Gaussian	0.200	0.200	0.215	0.200	0.191	0.147	0.207	0.200
Logistic	0.200	0.200	0.170	0.200	0.313	0.419	0.222	0.208

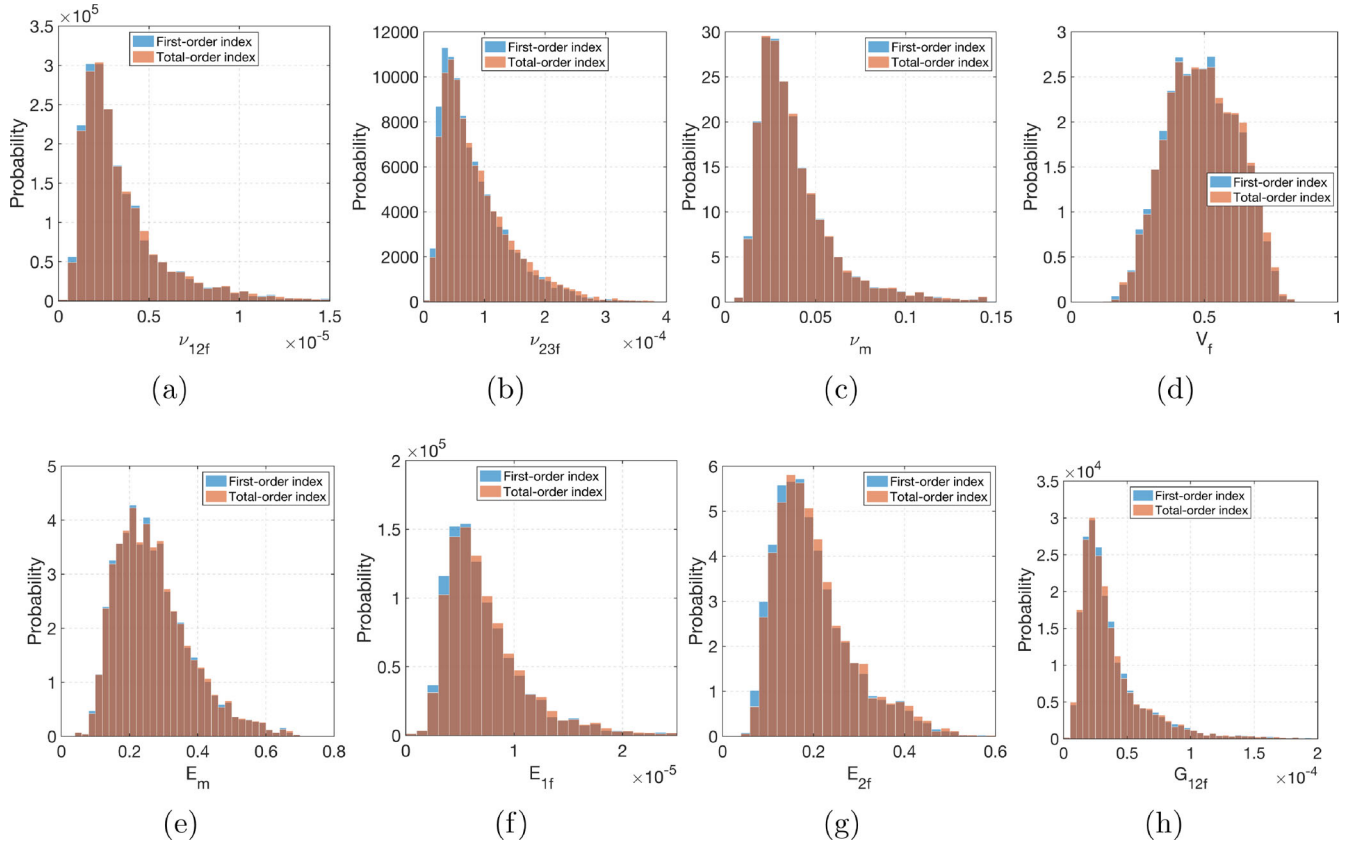
**Figure 4.** Ensemble of 500 candidate target probability distributions (gray curves) and optimal sampling density (black curves) for (a)  $\nu_{12f}$ , (b)  $\nu_{23f}$ , (c)  $\nu_m$ , (d)  $V_f$ , (e)  $E_m$ (GPa), (f)  $E_{1f}$ (GPa), (g)  $E_{2f}$ (GPa), and (h)  $G_{12f}$ (GPa).

exploring the effect of dimension reduction on the probabilistic prediction of composite elastic properties.

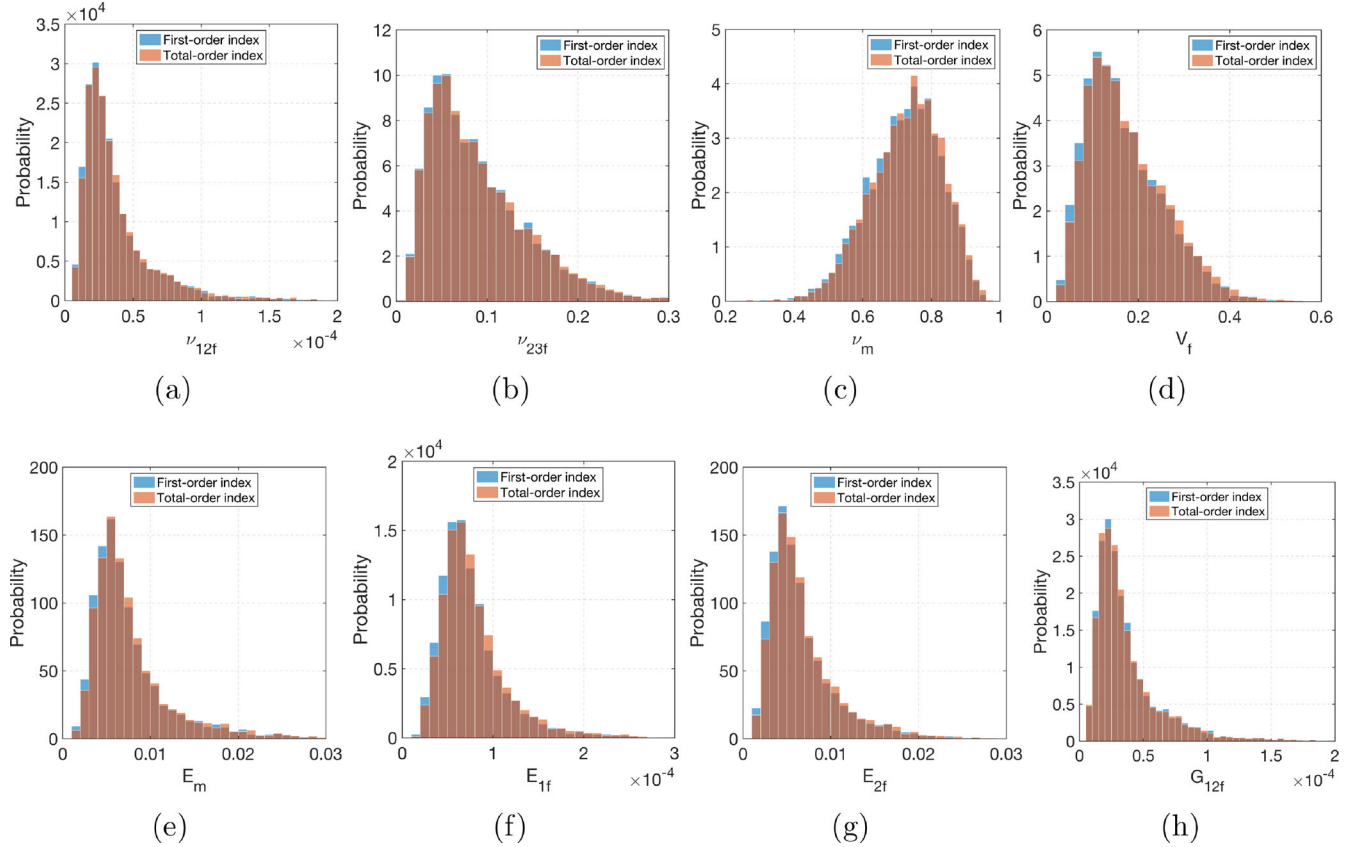
Figure 7 presents the complete probabilistic prediction for  $E_2$  as a set of empirical cumulative distribution functions (CDFs) with all eight random variables considered. As was the case for estimating imprecise Sobol indices, a total of 5000 joint target distributions are selected to represent the set of distributions. Then we draw 50,000 random samples from the optimal sampling density of each material property and reweight these samples to achieve efficient uncertainty propagation. The cloud of CDFs shows a large variation in  $E_2$  ranging from approximately 6 to 13 GPa. The high uncertainties inherent in the wide band of CDFs are caused by the lack of sufficient statistical data in each material property.

The computational results are compared to a statistical data set obtained from MIL-HDBK-17-2F [89]. The mean (8.27 GPa) and coefficient of variance (8.9) were determined from the experimental testing of 9 specimens from 3 batches of an AS4/3501-6 unidirectional lamina with a  $V_f$  of 0.54-0.55. These data were converted to a normal distribution and plotted in Figure 1. The experimental data falls slightly to the left of the predicted CDFs, most likely due to the lower  $V_f$  of the experimentally tested lamina than that of the computational simulation (mean  $V_f = 0.6$ ).

Figure 8 illustrates the probabilistic prediction for  $E_2$  with dimension reduction with the experimental data plotted for comparison. If only the most important variable,  $V_f$ , is considered for probabilistic prediction (see Figure 8a), the set of



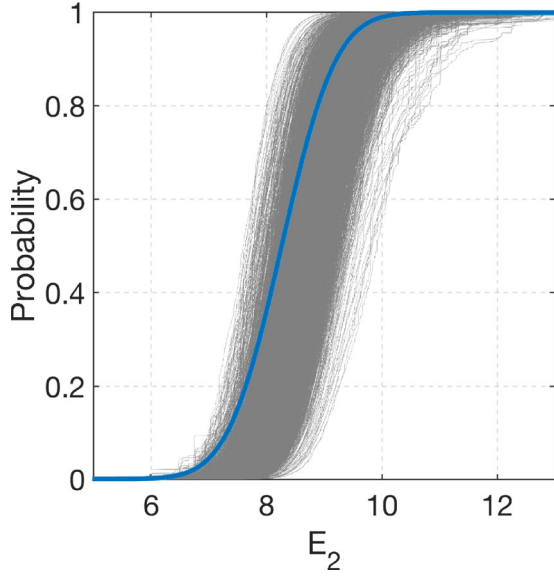
**Figure 5.** Histogram of first-order and total-order Sobol indices for  $E_2$  (GPa): (a)  $\nu_{12f}$ , (b)  $\nu_{23f}$ , (c)  $\nu_m$ , (d)  $V_f$ , (e)  $E_m$  (GPa), (f)  $E_{1f}$  (GPa), (g)  $E_{2f}$  (GPa), and (h)  $G_{12f}$  (GPa).



**Figure 6.** Histogram of first-order and total-order Sobol indices for  $\nu_{23}$ : (a)  $\nu_{12f}$ , (b)  $\nu_{23f}$ , (c)  $\nu_m$ , (d)  $V_f$ , (e)  $E_m$  (GPa), (f)  $E_{1f}$  (GPa), (g)  $E_{2f}$  (GPa), and (h)  $G_{12f}$  (GPa).



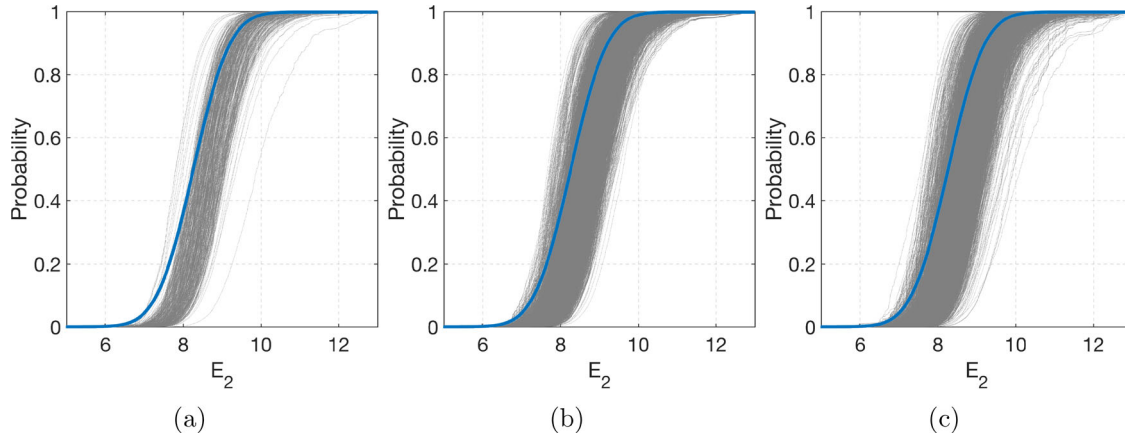
CDFs is much narrower than when considering all eight variables. Only the uncertainty associated with the top variable is retained, and the other seven variables are fixed by



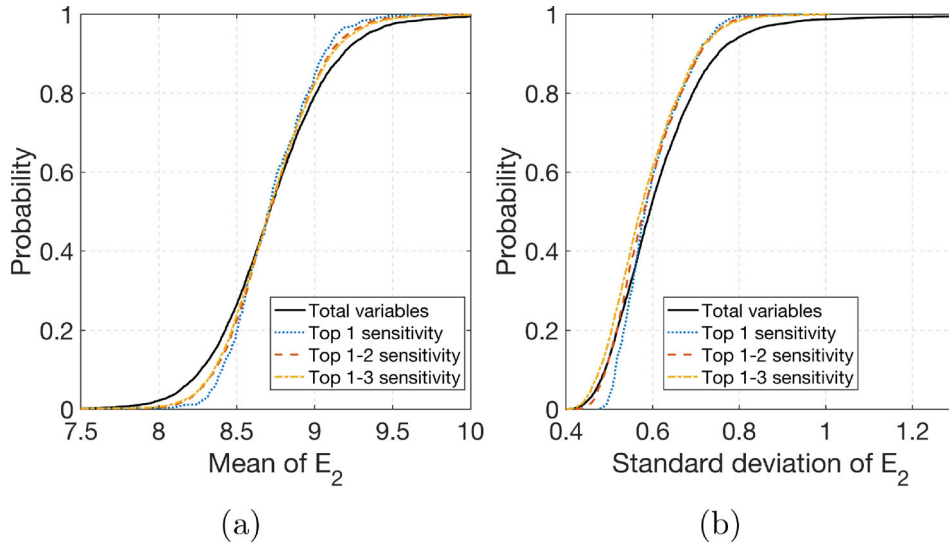
**Figure 7.** Empirical CDFs for  $E_2$  (GPa) considering all eight random variables. The blue line represents a set of experimental data for validation.

their mean values. When the top 2 variables are considered, the cloud of CDFs becomes much wider, as shown in Figure 8b. Meanwhile, the CDFs considering the top 3 variables are shown in Figure 8c and reflect almost the entire range of uncertainty in the CDFs as when all eight variables are considered.

We further compare the probabilistic prediction of the statistical mean and standard deviation of the elastic modulus  $E_2$ , as shown in Figure 9. Notice that the three lower-dimensional models show very similar CDFs for the mean and standard deviation as the full-dimensional model with all eight variables. To quantitatively compare the difference, a confidence interval metric is defined for the mean and standard deviation.  $\delta_{0.975}$  and  $\delta_{0.025}$  are defined as the upper bound and lower bound of the confidence level, respectively.  $\Delta_{0.95} = \delta_{0.975} - \delta_{0.025}$  is defined as the confidence interval and  $\lambda$  is defined as the ratio between the lower-dimensional model and full-dimensional model. Table 5 shows the confidence intervals for the mean and standard deviation of  $E_2$ . It is noted that the lower-dimensional models achieve a relatively high confidence interval ratio for the mean, ranging from 66.7% to 80.3%. The corresponding ratio of standard deviation ranges from 59.2% to 75.9%. In other words, by



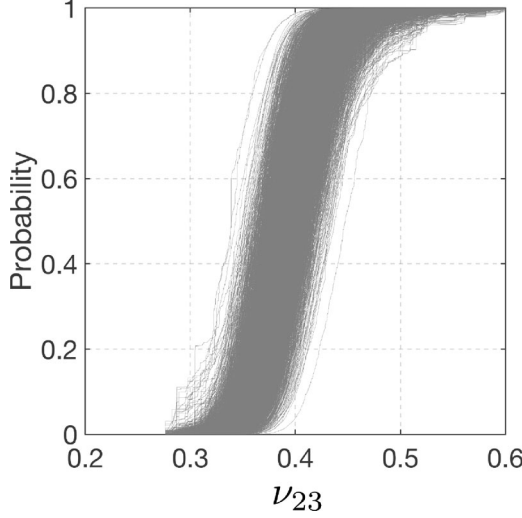
**Figure 8.** Empirical CDFs for  $E_2$  (GPa) considering only variations in the most important material properties (a) top 1 variable, (b) top 2 variables, and (c) top 3 variables.



**Figure 9.** Empirical CDFs for the mean and standard deviation of  $E_2$ .

**Table 5.** Confidence interval for the mean and standard deviation of  $E_2$ .

Confidence interval	Mean				Standard deviation			
	$\delta_{0.975}$	$\delta_{0.025}$	$\Delta_{0.95}$	$\lambda$ (%)	$\delta_{0.975}$	$\delta_{0.025}$	$\Delta_{0.95}$	$\lambda$ (%)
All 8 variables	9.494	8.023	1.47	100.00	0.891	0.453	0.437	100.00
Top 1 variable	9.277	8.296	0.981	66.70	0.756	0.497	0.259	59.20
Top 2 variables	9.328	8.188	1.14	77.60	0.77	0.465	0.305	69.80
Top 3 variables	9.354	8.173	1.181	80.30	0.776	0.444	0.332	75.90

**Figure 10.** Empirical CDFs for  $\nu_{23}$  considering all eight random variables.

reducing the dimension, the 95% confidence range of the probabilistic predictions reduces by approximately 20% for the mean value and 25% for the standard deviation.

Figure 10 shows empirical CDFs for probabilistic prediction of  $\nu_{23}$  considering all eight variables. It can be observed that the variation of  $\nu_{23}$  ranges from 0.28 to 0.6 (stretching into the range of unrealistic values for this physical property). Again, the wide band of CDFs results from the large uncertainties created by limited data in each material property. Statistical experimental data for  $\nu_{23}$  was not available in the literature for comparison, as this property is typically set equal to  $\nu_{12}$  and is challenging to physically test. Given that the calculation of  $\nu_{23}$  from the computational results is performed in the same manner as  $E_2$ , it can be reasonably assumed that the model is also validated for the prediction of  $\nu_{23}$ . The three lower-dimensional models shown in Figure 11 provide the CDFs for probabilistic prediction of  $\nu_{23}$  considering the reduced set of material properties. Similar to the  $E_2$  prediction, the lower-dimensional model built with only the single most important variable shows a much narrower band for the CDFs, but the top 3 variables case presents a nearly consistent cloud of CDFs as the full-dimensional model.

Empirical CDFs for the mean and standard deviation of  $\nu_{23}$  are shown in Figure 12. Lower dimensional models show a similar trend to the full-dimensional model. A quantitative comparison can be performed via the confidence interval, as shown in Table 6. The confidence interval ratio for the mean ranges from 47.1% to 88.9% and for the standard deviation changes from 78.7% to 87%. Compared with the elastic modulus, the Poisson's ratio here shows a higher confidence interval ratio, which is close to 90% when considering the three top variables. Using the IGSA approach,

the model dimension is effectively reduced from eight to three, while still retaining relatively high accuracy in the statistical bounds of the mean and standard deviation.

---

**Algorithm 1.** Probabilistic prediction with dimensionality-reduced model

---

- 1: Collect initial limited data  $\mathbf{d}_p$  for each random model input
  - 2: **for**  $i \leftarrow 1$  to  $d$  **do**
  - 3:   Identify candidate model set  $\mathcal{M}^i = \{M_j^i\}, j = 1, \dots, N_p$
  - 4:   Compute the posterior model probabilities  $\hat{\pi}_j^i$  using Bayesian multimodel inference
  - 5:   Estimate the posterior parameter densities  $p_i(\theta_j | \mathbf{d}_s, M_j)$  using MCMC
  - 6:   Establish a finite model set  $\mathcal{P}^i = \{\mathcal{P}_n^i\}, n = 1, \dots, N_r$  by random sampling
  - 7:   Determine the optimal sampling density  $q_i^*(\mathbf{x})$  through optimization
  - 8:   Draw i.i.d random samples  $\mathbf{x}_i \sim q_i^*(\mathbf{x})$  and  $\xi_i \sim q_i^*(\xi)$
  - 9:   Calculate the importance weights  $w_i(\mathbf{x}_i) = \frac{p_i(\mathbf{x}_i)}{q_i^*(\mathbf{x}_i)}$  and  $w_i(\xi_{-i}) = \frac{p_i(\xi_{-i})}{q_i^*(\xi_{-i})}$
  - 10: **end for**
  - 11: Evaluate the computational model  $f(\mathbf{x}), f(\xi)$  and  $f(\mathbf{x}_i, \xi_{-i})$
  - 12: Calculate the joint importance weights  $w(\mathbf{x})$  and  $w(\xi_{-i})$
  - 13: **for**  $l \leftarrow 1$  to  $N_r^d$  **do**
  - 14:   Reweight the random samples  $\mathbf{x}$  and  $\xi_{-i}$  by the importance weights  $w(\mathbf{x})$  and  $w(\xi_{-i})$
  - 15:   Calculate the first-order indices  $S_i^l$  and total-order indices  $S_i^{Tl}, i = 1, \dots, d$
  - 16: **end for**
  - 17: Evaluate the relative importance and interaction by analyzing  $S_i$  and  $S_i^T$
  - 18: Identify the top  $d_t$  ( $d_t < d$ ) random input variables with high sensitivity indices
  - 19: Reduce the dimensionality from  $d$  to  $d_t$  and fix the value for other model inputs
  - 20: **if** additional data  $\mathbf{d}^*$  are collected **then**
  - 21:    $\mathbf{d}_s = \mathbf{d}_s + \mathbf{d}^*$  and **goto** step 2
  - 22: **end if**
- 

## 7. Conclusion

This study investigates the effect of uncertainties associated with limited data for dimension reduction and probabilistic prediction of out-of-plane unidirectional composite lamina properties. An effective Bayesian approach is presented to estimate the uncertainties resulting from limited data in each material property. Both model-form and model parameter uncertainties are assessed by Bayesian uncertainty estimation. An ensemble of candidate target densities is then established to represent the imprecise probabilities in the assignment of model input variables (constituent material properties). Importance sampling reweighting is employed to efficiently propagate the uncertainties through the computational model and ultimately obtain a fully probabilistic prediction of the composite properties.

Within this probabilistic analysis framework, an effective method is presented to estimate the imprecise sensitivity indices and further reduce the model dimensionality. Based

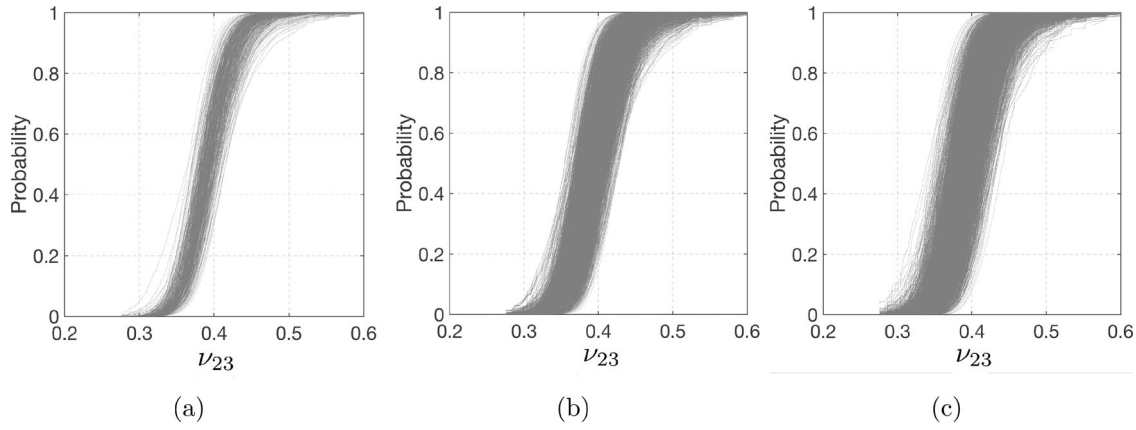


**Figure 11.** Empirical CDFs for  $\nu_{23}$  considering only variations in the most important material properties (a) top 1 variable, (b) top 2 variables, and (c) top 3 variables.

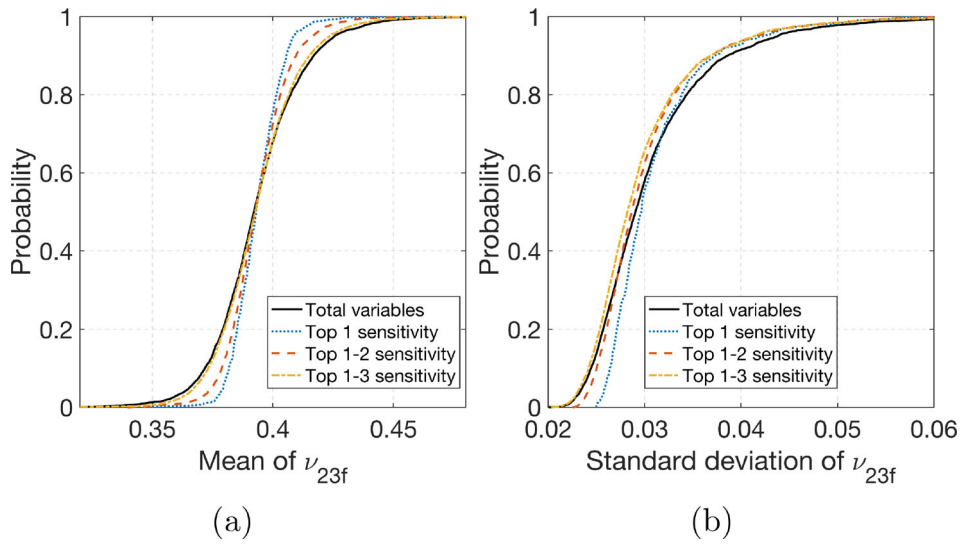


**Figure 12.** Empirical CDFs for the mean and standard deviation of  $\nu_{23}$ .

**Table 6.** Confidence intervals for the mean and standard deviation of  $\nu_{23}$ .

	Mean				Standard deviation			
Confidence interval	$\delta_{0.975}$	$\delta_{0.025}$	$\Delta_{0.95}$	$\lambda$ (%)	$\delta_{0.975}$	$\delta_{0.025}$	$\Delta_{0.95}$	$\lambda$ (%)
Total variables	0.437	0.359	0.078	100.00	0.049	0.023	0.026	100.00
Top 1variable	0.414	0.377	0.037	47.10	0.046	0.026	0.021	78.70
Top 1-2variables	0.422	0.37	0.052	66.80	0.046	0.024	0.022	85.90
Top 1-3variables	0.432	0.362	0.07	88.90	0.045	0.023	0.023	87.00

on the variance-based sampling method for Sobol index estimation, a novel importance sampling-based formulation is proposed to efficiently quantify imprecision in the Sobol indices. The developed algorithm therefore achieves simultaneous estimates of the first-order and total-order Sobol indices given an ensemble of candidate target distributions at a low computational cost, when compared to the traditional Monte Carlo method which requires multiple loops. Through the efficient IGSA approach, we can first identify the interaction among all random variables and second rank the input variables according to their relative importance. As a result, the model dimension reduction is achieved by varying only the most important variables instead of all of the model parameters.

Finally, the proposed approach is applied for probabilistic prediction of out-of-plane properties of a transversely




isotropic AS4/3501-6 unidirectional lamina given extremely sparse data to define constituent properties. In particular, it is shown that there is no strong interaction among all constituent properties in terms of the out-of-plane composite elastic properties. The elastic modulus depends strongly on the volume fraction, matrix elastic modulus as well as fiber elastic modulus along the 2 direction. The other constituent properties play only a minor role on the prediction. Using only these top 3 important variables as a lower-dimensional model, the proposed method presents comparable probabilistic predictions to the full dimensional model. A similar investigation of the out-of-plane Poisson's ratio indicates that volume fraction, matrix Poisson's ratio, and fiber Poisson's ratio in 2-3 account for nearly all variability. In this case, the lower-dimensional model achieves a relative high

prediction accuracy (close to 90%) in bounding the statistical mean and standard deviation.

## Funding

The work presented herein has been supported by the Office of Naval Research under Award Number N00014-16-1-2582 and N00014-16-1-2370 with Dr. Paul Hess as the program manager. The work of J. Zhang was supported by the U.S. Department of Energy, Office of Science, Office of Advanced Scientific Computing Research, Applied Mathematics program under contract ERKJ352; and by the Artificial Intelligence Initiative at the Oak Ridge National Laboratory (ORNL). ORNL is operated by UT-Battelle, LLC., for the U.S. Department of Energy under Contract DEAC05-00OR22725.

## ORCID

Jiabin Zhang  <http://orcid.org/0000-0002-7576-6110>  
 Michael Shields  <http://orcid.org/0000-0003-1370-6785>  
 Stephanie TerMaath  <http://orcid.org/0000-0003-0616-0980>

## References

- [1] N.R. Council, et al., Integrated Computational Materials Engineering: A Transformational Discipline for Improved Competitiveness and National Security, National Academies Press, Washington, DC, 2008.
- [2] J.H. Panchal, S.R. Kalidindi, and D.L. McDowell, Key computational modeling issues in integrated computational materials engineering, *Comput-Aided. Des.*, vol. 45, no. 1, pp. 4–25, 2013. DOI: [10.1016/j.cad.2012.06.006](https://doi.org/10.1016/j.cad.2012.06.006).
- [3] H. Dehmous, F. Duco, M. Karama, and H. Welemane, Multilevel assessment method for reliable design of composite structures, *Mech. Adv. Mater. Struct.*, vol. 24, no. 6, pp. 449–457, 2017. DOI: [10.1080/15376494.2016.1142027](https://doi.org/10.1080/15376494.2016.1142027).
- [4] S. Mahoney and J. Stiller, Towards a probabilistic framework for integrated computational materials engineering, In: 53rd AIAA/ASME/ASCE/AHS/ASC Structures, Structural Dynamics and Materials Conference 20th AIAA/ASME/AHS Adaptive Structures Conference 14th AIAA, p. 1529, Honolulu, HI, 2012. DOI: [10.2514/6.2012-1529](https://doi.org/10.2514/6.2012-1529).
- [5] S. Mukherjee, R. Ganguli, and S. Gopalakrishnan, Optimization of laminated composite structure considering uncertainty effects, *Mech. Adv. Mater. Struct.*, vol. 26, no. 6, pp. 493–502, 2019. DOI: [10.1080/15376494.2017.1400621](https://doi.org/10.1080/15376494.2017.1400621).
- [6] X. Xu, H. Yang, R. Augello, and E. Carrera, Optimized free-form surface modeling of point clouds from laser-based measurement, *Mech. Adv. Mater. Struct.*, pp. 1–9, 2019.
- [7] D. Blacketter, D. Walrath, and A. Hansen, Modeling damage in a plain weave fabric-reinforced composite material, *J. Compos. Technol. Res.*, vol. 15, no. 2, pp. 136–142, 1993. DOI: [10.1520/CTR10364J](https://doi.org/10.1520/CTR10364J).
- [8] K. Gipple and D. Hoyns, Measurement of the out-of-plane shear response of thick section composite materials using the v-notched beam specimen, *J. Compos. Mater.*, vol. 28, no. 6, pp. 543–572, 1994. DOI: [10.1177/002199839402800604](https://doi.org/10.1177/002199839402800604).
- [9] C. Sun and R. Vaidya, Prediction of composite properties from a representative volume element, *Compos. Sci. Technol.*, vol. 56, no. 2, pp. 171–179, 1996. DOI: [10.1016/0266-3538\(95\)00141-7](https://doi.org/10.1016/0266-3538(95)00141-7).
- [10] T. King, D. Blacketter, D. Walrath, and D. Adams, Micromechanics prediction of the shear strength of carbon fiber/epoxy matrix composites: the influence of the matrix and interface strengths, *J. Compos. Mater.*, vol. 26, no. 4, pp. 558–573, 1992. DOI: [10.1177/002199839202600406](https://doi.org/10.1177/002199839202600406).
- [11] C.C. Chamis, Simplified composite micromechanics equations for hygral, thermal and mechanical properties, NASA Technical Memorandum 83320, 38th Ann. Conf. of the Society of the Plastics Industry (SPI) Reinforced Plastics/Composites Inst.; February 07, 1983 - February 11, Houston, TX; United States, 1983.
- [12] P. Soden, M. Hinton, and A. Kaddour, Lamina properties, lay-up configurations and loading conditions for a range of fibre reinforced composite laminates. In: *Failure Criteria in Fibre-Reinforced-Polymer Composites*, Elsevier, Amsterdam, 2004. pp. 30–51.
- [13] P. Soden, M. Hinton, and A. Kaddour, Biaxial test results for strength and deformation of a range of e-glass and carbon fibre reinforced composite laminates: failure exercise benchmark data. In: *Failure Criteria in Fibre-Reinforced-Polymer Composites*, Elsevier, Amsterdam, 2004. pp. 52–96.
- [14] S.W. Tsai, *Composites design*, Vol. 5, Think Composites, Dayton, OH, 1988.
- [15] X. Xu, R. Augello, and H. Yang, The generation and validation of a cuf-based fea model with laser-based experiments, *Mech. Adv. Mater. Struct.*, pp. 1–8, 2019.
- [16] H. Yang and X. Xu, Multi-sensor technology for b-spline modelling and deformation analysis of composite structures, *Compos. Struct.*, vol. 224, pp. 111000, 2019. DOI: [10.1016/j.compstruct.2019.111000](https://doi.org/10.1016/j.compstruct.2019.111000).
- [17] H. Yang, X. Xu, B. Kargoll, and I. Neumann, An automatic and intelligent optimal surface modeling method for composite tunnel structures, *Compos. Struct.*, vol. 208, pp. 702–710, 2019. DOI: [10.1016/j.compstruct.2018.09.082](https://doi.org/10.1016/j.compstruct.2018.09.082).
- [18] A. Shaw, S. Sriramula, P.D. Gosling, and M.K. Chryssanthopoulos, A critical reliability evaluation of fibre reinforced composite materials based on probabilistic micro and macro-mechanical analysis, *Compos B: Eng.*, vol. 41, no. 6, pp. 446–453, 2010. DOI: [10.1016/j.compositesb.2010.05.005](https://doi.org/10.1016/j.compositesb.2010.05.005).
- [19] M.A. Alazwari and S.S. Rao, Interval-based uncertainty models for micromechanical properties of composite materials, *J. Reinf. Plast. Compos.*, vol. 37, no. 18, pp. 1142–1162, 2018. DOI: [10.1177/0731684418788733](https://doi.org/10.1177/0731684418788733).
- [20] S. Sriramula and M.K. Chryssanthopoulos, Quantification of uncertainty modelling in stochastic analysis of frp composites, *Compos A: Appl Sci Manuf.*, vol. 40, no. 11, pp. 1673–1684, 2009. DOI: [10.1016/j.compositesa.2009.08.020](https://doi.org/10.1016/j.compositesa.2009.08.020).
- [21] J. Aboudi, Micromechanical analysis of the strength of unidirectional fiber composites, *Compos. Sci. Technol.*, vol. 33, no. 2, pp. 79–96, 1988. DOI: [10.1016/0266-3538\(88\)90012-7](https://doi.org/10.1016/0266-3538(88)90012-7).
- [22] D.C. Charnpis, G.I. Schuëller, and M. Pellissetti, The need for linking micromechanics of materials with stochastic finite elements: A challenge for materials science, *Comput. Mater. Sci.*, vol. 41, no. 1, pp. 27–37, 2007. DOI: [10.1016/j.commatsci.2007.02.014](https://doi.org/10.1016/j.commatsci.2007.02.014).
- [23] R. Kriz and W. Stinchcomb, Elastic moduli of transversely isotropic graphite fibers and their composites, *Exp. Mech.*, vol. 19, no. 2, pp. 41–49, 1979. DOI: [10.1007/BF02324524](https://doi.org/10.1007/BF02324524).
- [24] P.C. Paul, C.R. Saff, K.B. Sanger, M.A. Mahler, H.-P. Kan, and E.F. Kautz, Analysis and test techniques for composite structures subjected to out-of-plane loads. In: *Composite Materials: Testing and Design (Tenth Volume)*, ASTM International, West Conshohocken, PA, 1992.
- [25] S.M. Serabian, The effects of nonlinear intralaminar shear behavior on the modeling accuracy of [(0/90) 3, 0] s and [(+45/-45) 3s pin-loaded laminates, *J. Compos. Technol. Res.*, vol. 13, no. 4, pp. 236–248, 1991. DOI: [10.1520/CTR10232J](https://doi.org/10.1520/CTR10232J).
- [26] R.H. Martin and W.C. Jackson, Damage prediction in cross-ply curved composite laminates. In: *Composite Materials: Fatigue and Fracture, Fourth Volume*, ASTM International, West Conshohocken, PA, 1993.
- [27] M. Sumich and K.T. Kedward, Development of a fatigue-life methodology for composite structures subjected to out-of-plane load components, Technical Report, NASA-TM-102885, 1991.
- [28] R.G. Rinaldi, M. Blacklock, H. Bale, M.R. Begley, and B.N. Cox, Generating virtual textile composite specimens using statistical data from micro-computed tomography: 3d tow



- representations, *J. Mech. Phys. Solids*, vol. 60, no. 8, pp. 1561–1581, 2012. DOI: [10.1016/j.jmps.2012.02.008](https://doi.org/10.1016/j.jmps.2012.02.008).
- [29] S. Banerjee and B.V. Sankar, Mechanical properties of hybrid composites using finite element method based micromechanics, *Compos B: Eng.*, vol. 58, pp. 318–327, 2014. DOI: [10.1016/j.compositesb.2013.10.065](https://doi.org/10.1016/j.compositesb.2013.10.065).
- [30] M.B. Goldsmith, B.V. Sankar, R.T. Haftka, and R.K. Goldberg, Effects of microstructural variability on thermo-mechanical properties of a woven ceramic matrix composite, *J. Compos. Mater.*, vol. 49, no. 3, pp. 335–350, 2015. DOI: [10.1177/0021998313519151](https://doi.org/10.1177/0021998313519151).
- [31] M. Komeili and A. Milani, The effect of meso-level uncertainties on the mechanical response of woven fabric composites under axial loading, *Comp. Struct.*, vol. 90, pp. 163–171, 2012. DOI: [10.1016/j.compstruct.2011.09.001](https://doi.org/10.1016/j.compstruct.2011.09.001).
- [32] T. Mukhopadhyay and S. Adhikari, Effective in-plane elastic moduli of quasi-random spatially irregular hexagonal lattices, *Int. J. Eng. Sci.*, vol. 119, pp. 142–179, 2017. DOI: [10.1016/j.ijengsci.2017.06.004](https://doi.org/10.1016/j.ijengsci.2017.06.004).
- [33] T. Mukhopadhyay and S. Adhikari, Stochastic mechanics of metamaterials, *Compos. Struct.*, vol. 162, pp. 85–97, 2017. DOI: [10.1016/j.compstruct.2016.11.080](https://doi.org/10.1016/j.compstruct.2016.11.080).
- [34] A. Carvalho, T. Silva, M.A.R. Loja, and F.R. Damásio, Assessing the influence of material and geometrical uncertainty on the mechanical behavior of functionally graded material plates, *Mech. Adv. Mater. Struct.*, vol. 24, no. 5, pp. 417–426, 2017. DOI: [10.1080/15376494.2016.1191100](https://doi.org/10.1080/15376494.2016.1191100).
- [35] S. Engelstad and J. Reddy, Probabilistic methods for the analysis of metal-matrix composites, *Compos. Sci. Technol.*, vol. 50, no. 1, pp. 91–107, 1994. DOI: [10.1016/0266-3538\(94\)90129-5](https://doi.org/10.1016/0266-3538(94)90129-5).
- [36] S. Engelstad and J. Reddy, Probabilistic nonlinear finite element analysis of composite structures, *AIAA J.*, vol. 31, no. 2, pp. 362–369, 1993. DOI: [10.2514/3.11676](https://doi.org/10.2514/3.11676).
- [37] B.V. Sankar and R.V. Marrey, Analytical method for micromechanics of textile composites, *Compos. Sci. Technol.*, vol. 57, no. 6, pp. 703–713, 1997. DOI: [10.1016/S0266-3538\(97\)00030-4](https://doi.org/10.1016/S0266-3538(97)00030-4).
- [38] X. Chen and Z. Qiu, A novel uncertainty analysis method for composite structures with mixed uncertainties including random and interval variables, *Compos. Struct.*, vol. 184, pp. 400–410, 2018. DOI: [10.1016/j.compstruct.2017.09.068](https://doi.org/10.1016/j.compstruct.2017.09.068).
- [39] T. Stock, P. Bellini, P. Murthy, and C. Chamis, Probabilistic composite micromechanics, In: *Advanced Marine Systems Conference*, San Diego, CA, p. 2375, 1988. DOI: [10.2514/6.1988-2375](https://doi.org/10.2514/6.1988-2375).
- [40] P.L. Murthy, S.K. Mital, and A.R. Shah, Probabilistic micromechanics/macromechanics for ceramic matrix composites, *J. Compos. Mater.*, vol. 32, no. 7, pp. 679–699, 1998. DOI: [10.1177/002199839803200705](https://doi.org/10.1177/002199839803200705).
- [41] S.S. Rao and Q. Liu, Fuzzy approach to the mechanics of fiber-reinforced composite materials, *AIAA J.*, vol. 42, no. 1, pp. 159–167, 2004. DOI: [10.2514/1.9039](https://doi.org/10.2514/1.9039).
- [42] H. Jeong and R. Shenoi, Probabilistic strength analysis of rectangular frp plates using monte carlo simulation, *CompStruct.*, vol. 76, no. 1-3, pp. 219–235, 2000. DOI: [10.1016/S0045-7949\(99\)00171-6](https://doi.org/10.1016/S0045-7949(99)00171-6).
- [43] S. Lin, Reliability predictions of laminated composite plates with random system parameters, *Probab. Eng. Mech.*, vol. 15, no. 4, pp. 327–338, 2000. DOI: [10.1016/S0266-8920\(99\)00034-X](https://doi.org/10.1016/S0266-8920(99)00034-X).
- [44] S. Sriramula and M.K. Chryssanthopoulos, Probabilistic models for spatially varying mechanical properties of in-service gfrp cladding panels, *J. Compos. Constr.*, vol. 13, no. 2, pp. 159–167, 2009. DOI: [10.1061/\(ASCE\)1090-0268\(2009\)13:2\(159\)](https://doi.org/10.1061/(ASCE)1090-0268(2009)13:2(159)).
- [45] A.-H. Zureick, R.M. Bennett, and B.R. Ellingwood, Statistical characterization of fiber-reinforced polymer composite material properties for structural design, *J. Struct. Eng.*, vol. 132, no. 8, pp. 1320–1327, 2006. DOI: [10.1061/\(ASCE\)0733-9445\(2006\)132:8\(1320\)](https://doi.org/10.1061/(ASCE)0733-9445(2006)132:8(1320)).
- [46] S. Sakata, F. Ashida, and M. Zako, Kriging-based approximate stochastic homogenization analysis for composite materials, *Comp Methods Appl Mech Eng.*, vol. 197, no. 21-24, pp. 1953–1964, 2008. DOI: [10.1016/j.cma.2007.12.011](https://doi.org/10.1016/j.cma.2007.12.011).
- [47] L. Sutherland and C.G. Soares, Review of probabilistic models of the strength of composite materials, *Reliab. Eng. Syst. Saf.*, vol. 56, no. 3, pp. 183–196, 1997. DOI: [10.1016/S0951-8320\(97\)00027-6](https://doi.org/10.1016/S0951-8320(97)00027-6).
- [48] C.C. Chamis, Probabilistic composite design. in: *Composite Materials: Testing and Design, Thirteenth Volume*, ASTM International, West Conshohocken, PA, 1997.
- [49] A. Saltelli, et al., *Global Sensitivity Analysis: The Primer*, John Wiley & Sons, Chichester, West Sussex, UK, 2008.
- [50] T. Homma and A. Saltelli, Importance measures in global sensitivity analysis of nonlinear models, *Reliab. Eng. Syst. Saf.*, vol. 52, no. 1, pp. 1–17, 1996. DOI: [10.1016/0951-8320\(96\)00002-6](https://doi.org/10.1016/0951-8320(96)00002-6).
- [51] H. Wang, L. Chen, F. Ye, and L. Chen, Global sensitivity analysis for fiber reinforced composite fiber path based on d-morph-hdmr algorithm, *Struct. Multidisc. Optim.*, vol. 56, no. 3, pp. 697–712, 2017. DOI: [10.1007/s00158-017-1681-9](https://doi.org/10.1007/s00158-017-1681-9).
- [52] J. Zhang and M.D. Shields, On the quantification and efficient propagation of imprecise probabilities resulting from small datasets, *Mech. Syst. Sig. Process.*, vol. 98, pp. 465–483, 2018. DOI: [10.1016/j.ymssp.2017.04.042](https://doi.org/10.1016/j.ymssp.2017.04.042).
- [53] J. Zhang, S. TerMaath, and M.D. Shields, Imprecise global sensitivity analysis using bayesian multimodel inference and importance sampling, *Reliability Engineering & System Safety* (in review), 2019.
- [54] Z. Hashin, Analysis of composite materials – a survey, *J Appl Mech.*, vol. 50, no. 3, pp. 481–505, 1983. DOI: [10.1115/1.3167081](https://doi.org/10.1115/1.3167081).
- [55] R. Hill, Elastic properties of reinforced solids: some theoretical principles, *J. Mech. Phys. Solids*, vol. 11, no. 5, pp. 357–372, 1963. DOI: [10.1016/0022-5096\(63\)90036-X](https://doi.org/10.1016/0022-5096(63)90036-X).
- [56] Z. Hashin and B.W. Rosen, The elastic moduli of fiber-reinforced materials, *J Appl Mech.*, vol. 31, no. 2, pp. 223–232, 1964. DOI: [10.1115/1.3629590](https://doi.org/10.1115/1.3629590).
- [57] T. Kanit, S. Forest, I. Galliet, V. Mounoury, and D. Jeulin, Determination of the size of the representative volume element for random composites: statistical and numerical approach, *Int. J. Solids Struct.*, vol. 40, no. 13/14, pp. 3647–3679, 2003. DOI: [10.1016/S0020-7683\(03\)00143-4](https://doi.org/10.1016/S0020-7683(03)00143-4).
- [58] Z. Xia, Y. Zhang, and F. Ellyin, A unified periodical boundary conditions for representative volume elements of composites and applications, *Int. J. Solids Struct.*, vol. 40, no. 8, pp. 1907–1921, 2003. DOI: [10.1016/S0020-7683\(03\)00024-6](https://doi.org/10.1016/S0020-7683(03)00024-6).
- [59] S. Swaminathan, S. Ghosh, and N. Pagano, Statistically equivalent representative volume elements for unidirectional composite microstructures: Part i-without damage, *J. Compos. Mater.*, vol. 40, no. 7, pp. 583–604, 2006. DOI: [10.1177/0021998305055273](https://doi.org/10.1177/0021998305055273).
- [60] L. Maragoni, P. Carraro, and M. Quaresimin, Development, validation and analysis of an efficient micro-scale representative volume element for unidirectional composites, *Compos A: Appl Sci Manuf.*, vol. 110, pp. 268–283, 2018. DOI: [10.1016/j.compositesa.2018.04.025](https://doi.org/10.1016/j.compositesa.2018.04.025).
- [61] A. Bahmani, G. Li, T.L. Willett, and J. Montesano, Three-dimensional microscopic assessment of randomly distributed representative volume elements for high fiber volume fraction unidirectional composites, *Compos. Struct.*, vol. 192, pp. 153–164, 2018. DOI: [10.1016/j.compstruct.2018.02.075](https://doi.org/10.1016/j.compstruct.2018.02.075).
- [62] D.V. Kubair and S. Ghosh, Statistics informed boundary conditions for statistically equivalent representative volume elements of clustered composite microstructures, *Mech. Adv. Mater. Struct.*, vol. 25, no. 14, pp. 1205–1213, 2018. DOI: [10.1080/15376494.2017.1330980](https://doi.org/10.1080/15376494.2017.1330980).
- [63] S. Li, General unit cells for micromechanical analyses of unidirectional composites, *Compos A: Appl. Sci Manuf.*, vol. 32, no. 6, pp. 815–826, 2001. DOI: [10.1016/S1359-835X\(00\)00182-2](https://doi.org/10.1016/S1359-835X(00)00182-2).
- [64] M.-J. Pindera, H. Khatam, A.S. Drago, and Y. Bansal, Micromechanics of spatially uniform heterogeneous media: a critical review and emerging approaches, *Compos B: Eng.*, vol. 40, no. 5, pp. 349–378, 2009. DOI: [10.1016/j.compositesb.2009.03.007](https://doi.org/10.1016/j.compositesb.2009.03.007).
- [65] L. Jeanmeure and S. Li, Automated generation of equation-based boundary conditions for multiscale modelling of unit cells. 18th International Conference on Composite Materials, 21th to 26th of August, 2011, Jeju Island, Korea.

- [66] S. Kurukuri, A comprehensive study: Boundary conditions for representative volume elements (rve) of composites. Institute of Structural Mechanics.
- [67] S. Li, Boundary conditions for unit cells from periodic microstructures and their implications, *Compos. Sci. Technol.*, vol. 68, no. 9, pp. 1962–1974, 2008. DOI: [10.1016/j.compscitech.2007.03.035](https://doi.org/10.1016/j.compscitech.2007.03.035).
- [68] V.-D. Nguyen, E. Béchet, C. Geuzaine, and L. Noels, Imposing periodic boundary condition on arbitrary meshes by polynomial interpolation, *Comput. Mater. Sci.*, vol. 55, pp. 390–406, 2012. DOI: [10.1016/j.commatsci.2011.10.017](https://doi.org/10.1016/j.commatsci.2011.10.017).
- [69] V. Buryachenko, *Micromechanics of Heterogeneous Materials*, Springer Science & Business Media, New York, NY, 2007.
- [70] J. Zhang and M.D. Shields, The effect of prior probabilities on quantification and propagation of imprecise probabilities resulting from small datasets, *Comp Methods Appl Mech Eng.*, vol. 334, pp. 483–506, 2018. DOI: [10.1016/j.cma.2018.01.045](https://doi.org/10.1016/j.cma.2018.01.045).
- [71] K.P. Burnham and D.R. Anderson, Multimodel inference understanding aic and bic in model selection, *Sociol Methods Res.*, vol. 33, no. 2, pp. 261–304, 2004. DOI: [10.1177/0049124104268644](https://doi.org/10.1177/0049124104268644).
- [72] L. Martino, V. Elvira, and F. Louzada, Effective sample size for importance sampling based on discrepancy measures, *Signal Process.*, vol. 131, pp. 386–401, 2017. DOI: [10.1016/j.sigpro.2016.08.025](https://doi.org/10.1016/j.sigpro.2016.08.025).
- [73] J. Zhang and M.D. Shields, Efficient monte carlo resampling for probability measure changes from bayesian updating, *Probab. Eng. Mech.*, vol. 55, pp. 54–66, 2019. DOI: [10.1016/j.probg-mech.2018.10.002](https://doi.org/10.1016/j.probg-mech.2018.10.002).
- [74] I.M. Sobol, Global sensitivity indices for nonlinear mathematical models and their monte carlo estimates, *Math. Comput. Simul.*, vol. 55, no. 1–3, pp. 271–280, 2001.
- [75] M. Stein, Large sample properties of simulations using latin hypercube sampling, *Technometrics*, vol. 29, no. 2, pp. 143–151, 1987. DOI: [10.1080/00401706.1987.10488205](https://doi.org/10.1080/00401706.1987.10488205).
- [76] M.D. Shields and J. Zhang, The generalization of latin hypercube sampling, *Reliab. Eng. Syst. Saf.*, vol. 148, pp. 96–108, 2016. DOI: [10.1016/j.ress.2015.12.002](https://doi.org/10.1016/j.ress.2015.12.002).
- [77] P. Soden, M. Hinton, and A. Kaddour, Lamina properties, lay-up configurations and loading conditions for a range of fibre reinforced composite laminates. In: *Composites Science and Technology*, Vol. 58, Elsevier, Oxford, UK, 1998. pp. 1011–1022 DOI: [10.1016/S0266-3538\(98\)00078-5](https://doi.org/10.1016/S0266-3538(98)00078-5).
- [78] G. Karami and M. Garnich, Effective moduli and failure considerations for composites with periodic fiber waviness, *Compos. Struct.*, vol. 67, no. 4, pp. 461–475, 2005. DOI: [10.1016/j.comp-struct.2004.02.005](https://doi.org/10.1016/j.comp-struct.2004.02.005).
- [79] J.H. Yim and J. Gillespie, Jr, Damping characteristics of 0 and 90 as4/3501-6 unidirectional laminates including the transverse shear effect, *Compos. Struct.*, vol. 50, no. 3, pp. 217–225, 2000. DOI: [10.1016/S0263-8223\(00\)00087-8](https://doi.org/10.1016/S0263-8223(00)00087-8).
- [80] D.M. Blackketter, D. Upadhyaya, and T. King, Micromechanics prediction of the transverse tensile strength of carobn fiber/epoxy composites: The influence of the matrix and interface, *Polym. Compos.*, vol. 14, no. 5, pp. 437–446, 1993. DOI: [10.1002/pc.750140511](https://doi.org/10.1002/pc.750140511).
- [81] D.F. Adams and L.G. Adams, Tensile impact tests of as4/3501-6 and s2/3501-6 unidirectional composites and the 3501-6 epoxy matrix, *J. Compos. Mater.*, vol. 24, no. 3, pp. 256–268, 1990. DOI: [10.1177/002199839002400302](https://doi.org/10.1177/002199839002400302).
- [82] M. Guagliano and E. Riva, Mechanical behaviour prediction in plain weave composites, *J Strain Anal Eng Design*, vol. 36, no. 2, pp. 153–162, 2001. DOI: [10.1243/0309324011512702](https://doi.org/10.1243/0309324011512702).
- [83] G. Nicoletto and E. Riva, Failure mechanisms in twill-weave laminates: Fem predictions vs. experiments, *Compos A: Appl Sci Manuf.*, vol. 35, no. 7-8, pp. 787–795, 2004. DOI: [10.1016/j.compositesa.2004.01.007](https://doi.org/10.1016/j.compositesa.2004.01.007).
- [84] H. Composites, 3501-6 epoxy matrix, Product Data, 1998.
- [85] I.M. Daniel and O. Ishai, *Engineering Mechanics of Composite Materials*, Vol. 3, Oxford University Press New York, 1994. DOI: [10.1086/ahr/99.4.1289](https://doi.org/10.1086/ahr/99.4.1289).
- [86] M. Baucio, *ASM Engineered Materials Reference Book*, ASM International, Materials Park, OH, 1994.
- [87] M. Kutz, *Handbook of Materials Selection*, John Wiley & Sons, New York, NY, 2002.
- [88] P.K. Mallick, *Composites Engineering Handbook*, CRC Press, 1997.
- [89] MIL-HDBK-17-2F, In: *Department of Defense Composite Materials Handbook*, Vol. 2, Polymer Matrix Composites Materials Properties, 2002.